

Independent-particle theory of the Franz-Keldysh effect including interband coupling: Application to calculation of electroabsorption in GaAs

J. K. Wahlstrand* and J. E. Sipe†

JILA, National Institute of Standards and Technology, and University of Colorado, Boulder, Colorado 80309, USA

(Received 22 April 2010; revised manuscript received 27 June 2010; published 9 August 2010)

We calculate the linear optical absorption spectrum for a semiconductor in the presence of a strong constant (dc) electric field (the Franz-Keldysh effect). An independent particle theory is developed that treats the dc field nonperturbatively and the optical field perturbatively. Results are presented from a calculation using a 14-band $\mathbf{k}\cdot\mathbf{p}$ model for the band structure of GaAs that includes remote band effects to order k^2 . We also include remote band effects in the matrix elements for consistency. Coupling between nearly degenerate bands due to the dc field plays an important role, both near the valence band degeneracy in the center of the Brillouin zone and along lines where spin-split bands become degenerate. We calculate the electroabsorption spectrum with a dc field pointing along various crystal directions and predict experimentally accessible effects due to band warping. Calculations using the 14-band model show a change in the absorption spectrum that depends on the sign of the electric field, reflecting the lack of a center of inversion symmetry in GaAs. The theoretical framework presented can be easily extended to nonlinear absorption.

DOI: [10.1103/PhysRevB.82.075206](https://doi.org/10.1103/PhysRevB.82.075206)

PACS number(s): 78.20.Jq, 71.20.-b, 78.66.Fd

I. INTRODUCTION

The Franz-Keldysh effect (FKE) is the modification of the optical properties of a semiconductor caused by the interaction of photoexcited carriers with a static electric field.¹⁻⁴ For light with energy below the band gap, the electric field enables absorption through tunneling, producing an exponential tail in the absorption spectrum, potentially useful in optical modulators.⁵ For light with energy above the band gap, coherent acceleration of photoexcited carriers leads to Franz-Keldysh oscillations. In the presence of lifetime broadening and decoherence, the oscillations are damped, but there remains an enhanced signal at band structure critical points.⁶ This forms the basis for electroreflectance and electroabsorption, widely used techniques for studying the electronic structure of materials. Analysis of Franz-Keldysh oscillations has also been used as a way of determining effective masses in new materials and heterostructures.⁷

An analytical theory³ based on the parabolic band approximation (PBA) has been found to be consistent with most experiments. There the absorption spectrum can be expressed in terms of Airy functions, and the Franz-Keldysh oscillation period is simply related to the effective mass and electric field strength. The oscillation period has been shown to be remarkably robust against the effects of nonparabolicity.^{8,9} Where bands become degenerate, such as near the Γ point for the uppermost valence bands in GaAs, interband coupling caused by the electric field seriously complicates the theory, but it has been found that to a good approximation the contributions of the bands can be calculated separately as if they are uncoupled, and then simply summed.^{10,11} Numerical calculations of the FKE using model band structures have been performed,^{8,12} but, perhaps because of the qualitative agreement between the PBA theory and experiment, the effects of band structure on the FKE have not received much attention.

Our goal here is to set up a complete formalism appropriate for describing the FKE within the independent particle

approximation. We treat band structure effects essentially exactly and to all orders in the applied dc field; while in our example calculations we will use simple model band structures, the formalism we develop could be applied utilizing full band structure calculations over the entire Brillouin zone. We perturbatively treat the optical field, and consider both the effect of short pulses of light, where the total density of carriers injected is the relevant quantity to be calculated, and the effect of continuous radiation, where a Fermi's golden rule expression for the rate at which a density of carriers is injected is the quantity of interest. Although our focus in this paper is on one-photon absorption as modified by the dc field, and hence the usual FKE, the approach we take is easily generalized to other absorption processes, such as two-photon and higher absorption, and interferences between such processes. The formalism is structured in such a way that it illustrates how the dc field leads to modifications in the familiar, dc field free expressions.

We use the framework to calculate electroabsorption in GaAs using a 14-band $\mathbf{k}\cdot\mathbf{p}$ model for the band structure. We find that the coupling induced by the electric field between nearly degenerate bands near the Γ point and along high symmetry directions is extremely important. If it is neglected, the strong variation of the matrix element phase resulting from the near degeneracy causes an extremely distorted spectrum that is inconsistent with experiment. While the role of degeneracy in the FKE near the Γ point in zincblende semiconductors has been discussed previously,^{8,10-14} the importance of interactions near lines of degeneracy in models with spin splitting was not previously recognized. We feel that the general importance of the strong coupling between degenerate bands in the FKE is not widely appreciated so we discuss it in detail here.

A major limitation of our approach, of course, is the neglect of carrier-carrier interactions. Both excitonic effects associated with the electron-hole interaction,^{15,16} and more subtle effects due to decoherence of the Bloch states¹⁷ caused by interactions with phonons and other electrons, are ne-

glected. Our interest in the FKE is driven in part by the way it may serve as a probe of such phenomena. Before attacking the treatment of these effects, however, we feel it is important to place the treatment at the independent-particle level on a firm and modern footing so that the consequences of including more complicated effects can accurately be identified.

II. THEORETICAL FRAMEWORK

In this section we sketch out the theory. The strategy is a usual one; we move into an interaction picture to make the calculation of the absorption of light, where the Hamiltonian in the interaction picture is only nonzero when the optical field is present. The details are slightly more complicated than usual because we must treat the optical field in the presence of a dc field and all its effects, including the coupling between different bands. Hence we delegate some of the details to the appendices.

A. Hamiltonian and basis states

In the independent particle approximation, with the usual assumption of an interaction of the charges with a classically described electromagnetic field in the long-wavelength limit, the dynamics of the system of charges is described by the Hamiltonian

$$H(t) = \int \psi^\dagger(\mathbf{x}) \mathcal{H}(t) \psi(\mathbf{x}) d\mathbf{x}, \quad (1)$$

where

$$\mathcal{H}(t) = \frac{1}{2m} \left[\frac{\hbar}{i} \nabla - \frac{e}{c} \mathbf{A}(t) \right]^2 + V(\mathbf{x}) \quad (2)$$

and where $\psi(\mathbf{x})$ is the electron field operator (in the Schrödinger picture), satisfying the anticommutation relations

$$\{\psi(\mathbf{x}), \psi^\dagger(\mathbf{x}')\} = \delta(\mathbf{x} - \mathbf{x}'). \quad (3)$$

The term $V(\mathbf{x})$ describes the interaction of the charges with the periodically arranged ions in the crystal and any part of the electron-electron interaction that can be included in an effective time-independent single particle potential.

The vector potential $\mathbf{A}(t) = \mathbf{A}_{dc}(t) + \mathbf{A}_{opt}(t)$ describes both the optical field

$$\mathbf{E}_{opt}(t) = -\frac{1}{c} \frac{\partial \mathbf{A}_{opt}(t)}{\partial t}, \quad (4)$$

which we assume to be an optical pulse centered at $t=0$ with zero amplitude after some time $t_{end} > 0$ and a nominal dc field

$$\mathbf{E}_{dc}(t) = -\frac{1}{c} \frac{\partial \mathbf{A}_{dc}(t)}{\partial t} \quad (5)$$

that we assume is turned on and then held constant after some initial time $t_{initial} < 0$. Putting

$$\mathbf{K}(t) = -\frac{e}{\hbar c} \mathbf{A}_{dc}(t) \quad (6)$$

and neglecting a term proportional to \mathbf{A}_{opt}^2 , whose effects can be absorbed in a phase factor of the total wave function, Eq. (2) can be written as

$$\mathcal{H}(t) = \mathcal{H}_{dc}(t) - \frac{e}{mc} \left[\frac{\hbar}{i} \nabla + \hbar \mathbf{K}(t) \right] \cdot \mathbf{A}_{opt}(t), \quad (7)$$

where

$$\mathcal{H}_{dc}(t) = \frac{1}{2m} \left[\frac{\hbar}{i} \nabla + \hbar \mathbf{K}(t) \right]^2 + V(\mathbf{x}).$$

The usual Bloch functions $\phi_n(\mathbf{k}; \mathbf{x})$, labeled by band index n and crystal wavevector \mathbf{k} , satisfy

$$\mathcal{H}_0 \phi_n(\mathbf{k}; \mathbf{x}) = \hbar \omega_n(\mathbf{k}) \phi_n(\mathbf{k}; \mathbf{x}), \quad (8)$$

where

$$\mathcal{H}_0 = \frac{1}{2m} \left(\frac{\hbar}{i} \nabla \right)^2 + V(\mathbf{x}).$$

They can be written as $\phi_n(\mathbf{k}; \mathbf{x}) = \Omega^{-1/2} u_n(\mathbf{k}; \mathbf{x}) e^{i\mathbf{k} \cdot \mathbf{x}}$, with $u_n(\mathbf{k}; \mathbf{x} + \mathbf{R}) = u_n(\mathbf{k}; \mathbf{x})$, where \mathbf{R} is a lattice vector; Ω is the normalization volume. We deal here only with simple band topologies where points and lines of degeneracy in reciprocal space exist, but no planes of degeneracy. Then the $\phi_n(\mathbf{k}; \mathbf{x})$ can be well-defined in reciprocal space at all \mathbf{k} , except where there is degeneracy, by requiring periodicity in the lattice vectors, i.e., $\phi_n(\mathbf{k} + \mathbf{G}; \mathbf{x}) = \phi_n(\mathbf{k}; \mathbf{x})$ and $\omega_n(\mathbf{k} + \mathbf{G}) = \omega_n(\mathbf{k})$, where \mathbf{G} is a reciprocal lattice vector, and taking¹⁸

$$i \frac{\partial u_n(\mathbf{k}; \mathbf{x})}{\partial \mathbf{k}} = \sum_m u_m(\mathbf{k}; \mathbf{x}) \xi_{mn}(\mathbf{k})$$

for points \mathbf{k} where the band n is nondegenerate. The $\xi_{mn}(\mathbf{k})$ satisfy $\xi_{mn}^*(\mathbf{k}) = \xi_{nm}(\mathbf{k})$, and for m and n nondegenerate at \mathbf{k} are given by

$$\xi_{mn}(\mathbf{k}) = \frac{\mathbf{v}_{mn}(\mathbf{k})}{i \omega_{mn}(\mathbf{k})},$$

where

$$\mathbf{v}_{mn}(\mathbf{k}) \equiv \frac{1}{m} \int \phi_m^*(\mathbf{k}; \mathbf{x}) \left(\frac{\hbar}{i} \nabla \right) \phi_n(\mathbf{k}; \mathbf{x}) d\mathbf{x}$$

and $\omega_{mn}(\mathbf{k}) = \omega_m(\mathbf{k}) - \omega_n(\mathbf{k})$. The phases of the $\xi_{mn}(\mathbf{k})$ ($m \neq n$) and the functions $\xi_{mm}(\mathbf{k})$ are chosen so that the periodicity conditions are satisfied.

Rather than using the set of states $\{\phi_n(\mathbf{k}; \mathbf{x})\}$ as an expansion basis for the field operator $\psi(\mathbf{x})$, it is more convenient to use a basis of instantaneous eigenstates of $\mathcal{H}_{dc}(t)$

$$\mathcal{H}_{dc}(t) \bar{\phi}_n(\mathbf{k}; \mathbf{x}) = \hbar \omega_n(\mathbf{k} + \mathbf{K}) \bar{\phi}_n(\mathbf{k}; \mathbf{x}) \quad (9)$$

leaving implicit the time dependence of \mathbf{K} and $\bar{\phi}_n(\mathbf{k}; \mathbf{x})$. A state $\bar{\phi}_n(\mathbf{k}; \mathbf{x})$ satisfying Eq. (9) is easily shown to be characterized by crystal momentum $\mathbf{k} + \mathbf{K}$. One way of constructing such a set $\{\bar{\phi}_n(\mathbf{k}; \mathbf{x})\}$, which forms a complete set of

states as n ranges over all band indices and \mathbf{k} ranges over one Brillouin zone, was discussed earlier by Sipe and Ghahramani,¹⁹ to which we refer for details. It is the approach we adopt here with a slight modification of the initial conditions. Before the dc field is turned on, from Eqs. (5) and (6) it is clear that $\mathbf{K}(t)$ must be a constant vector, which we write as \mathbf{K}^o

$$\mathbf{K}(t < t_{\text{initial}}) = \mathbf{K}^o.$$

We see from Eqs. (8) and (9) that we can take $\bar{\phi}_n(\mathbf{k}; \mathbf{x})$ to be $\phi_n(\mathbf{k} + \mathbf{K}^o; \mathbf{x})$, and therefore time independent. When the dc field is turned on, a prescription can be written down for constructing $\bar{\phi}_n(\mathbf{k}; \mathbf{x})$ at $t + dt$ given that the set $\{\bar{\phi}_n(\mathbf{k}; \mathbf{x})\}$ is known at t . That prescription involves first choosing to identify the degenerate states at \mathbf{k} at time t so that they satisfy $\mathbf{E}_{\text{dc}}(t) \cdot \mathbf{V}_{mn}(\mathbf{k}; t) = 0$ for states $m \neq n$, where

$$\mathbf{V}_{mn}(\mathbf{k}; t) \equiv \frac{1}{m} \int \bar{\phi}_m^*(\mathbf{k}; \mathbf{x}) \left(\frac{\hbar}{i} \nabla + \hbar \mathbf{K} \right) \bar{\phi}_n(\mathbf{k}; \mathbf{x}) d\mathbf{x} \quad (10)$$

and then determining the states at $t + dt$ in terms of those at t by using

$$i\hbar \frac{d\bar{\phi}_n(\mathbf{k}; \mathbf{x})}{dt} = \sum_m \bar{\phi}_m(\mathbf{k}; \mathbf{x}) \boldsymbol{\mu}_{mn}(\mathbf{k}; t) \cdot \mathbf{E}_{\text{dc}}(t), \quad (11)$$

where the sum excludes any states m degenerate with n and

$$\boldsymbol{\mu}_{mn}(\mathbf{k}; t) \equiv \frac{e\mathbf{V}_{mn}(\mathbf{k}; t)}{i\omega_{mn}(\mathbf{k} + \mathbf{K})}. \quad (12)$$

With proper caution for the labeling of band indices as $\mathbf{k} + \mathbf{K}$ moves through degeneracy points or lines, the resulting states $\bar{\phi}_n(\mathbf{k}; \mathbf{x})$ are found to be $\bar{\phi}_n(\mathbf{k}; \mathbf{x}) = \Omega^{-1/2} \bar{u}_n(\mathbf{k}; \mathbf{x}) e^{i\mathbf{k} \cdot \mathbf{x}}$, where $\bar{u}_n(\mathbf{k}; \mathbf{x}) = e^{-i\varphi_n(\mathbf{k}; t)} u_n(\mathbf{k} + \mathbf{K})$ with

$$\varphi_n(\mathbf{k}; t) = - \int_{\mathbf{k}}^{\mathbf{k} + \mathbf{K}(t)} \boldsymbol{\xi}_{nn}(\boldsymbol{\kappa}') \cdot d\boldsymbol{\kappa}' \quad (13)$$

and where the line integral is along a path determined by the evolution of $\mathbf{K}(t)$, taking

$$\boldsymbol{\kappa}' = \mathbf{k} + \mathbf{K}(t'). \quad (14)$$

Using these expressions we find

$$\mathbf{V}_{mn}(\mathbf{k}; t) = \mathbf{v}_{mn}[\mathbf{k} + \mathbf{K}(t)] e^{i\varphi_{mn}(\mathbf{k}; t)}, \quad (15)$$

where

$$\varphi_{mn}(\mathbf{k}; t) = \varphi_m(\mathbf{k}; t) - \varphi_n(\mathbf{k}; t). \quad (16)$$

Thus from Eq. (12) we have

$$\boldsymbol{\mu}_{mn}(\mathbf{k}; t) = e\mathbf{r}_{mn}[\mathbf{k} + \mathbf{K}(t)] e^{i\varphi_{mn}(\mathbf{k}; t)}, \quad (17)$$

where we have put

$$\begin{aligned} \mathbf{r}_{mn}(\mathbf{k}) &\equiv \boldsymbol{\xi}_{mn}(\mathbf{k}) \text{ if } \omega_m(\mathbf{k}) \neq \omega_n(\mathbf{k}), \\ &\equiv 0 \text{ if } \omega_m(\mathbf{k}) = \omega_n(\mathbf{k}) \end{aligned}$$

so that the sum in Eq. (11) can be formally taken to be unrestricted.

It is clear that a wave function $\bar{\phi}_n(\mathbf{k}; \mathbf{x})$ describes the adiabatic energy eigenstate of an electron in the presence of a dc field, including the effect of a Berry's phase described by the $\boldsymbol{\xi}_{mn}(\mathbf{k})$. Thus the set of states $\{\bar{\phi}_n(\mathbf{k}; \mathbf{x})\}$ form a natural basis in which to discuss the absorption in the presence of a dc field. From this point of view, it is because both the electron's initial and final states must be thought of as moving through the Brillouin zone during the time in which the electron is interacting with the optical field that the absorption spectrum in the presence of the dc field is different than in its absence.

However, the dc field can also induce transitions between the bands as the electrons move through them and this will affect the absorption of the optical field. To deal with this effect we work with time dependent states $\bar{\chi}_m(\mathbf{k}; \mathbf{x})$ that are in fact linear combinations of the $\{\bar{\phi}_n(\mathbf{k}; \mathbf{x})\}$ at each \mathbf{k} and t . We do this by introducing evolution matrices $L(\mathbf{k}; t)$, with elements $L_{pm}(\mathbf{k}; t)$, and write

$$\bar{\chi}_m(\mathbf{k}; \mathbf{x}) = \sum_p L_{pm}(\mathbf{k}; t) \bar{\phi}_p(\mathbf{k}; \mathbf{x}). \quad (18)$$

The matrices will be chosen to be unitary so from $LL^\dagger = I$ we have

$$\bar{\phi}_n(\mathbf{k}; \mathbf{x}) = \sum_m L_{nm}^*(\mathbf{k}; t) \bar{\chi}_m(\mathbf{k}; \mathbf{x}). \quad (19)$$

Just as the $\{\bar{\phi}_n(\mathbf{k}; \mathbf{x})\}$ form a complete and orthonormal set of (time dependent) states so do the $\{\bar{\chi}_m(\mathbf{k}; \mathbf{x})\}$. For times $t < t_{\text{initial}}$, when we have $\bar{\phi}_n(\mathbf{k}; \mathbf{x})$ independent of time and proportional to $\phi_n(\mathbf{k} + \mathbf{K}^o; \mathbf{x})$ [see the discussion after Eq. (9)], it will be convenient to take

$$L_{mp}(\mathbf{k}; t) = \delta_{mp} e^{-i\omega_m(\mathbf{k} + \mathbf{K}^o)t} \text{ for } t < t_{\text{initial}} \quad (20)$$

capturing the usual evolution of the Bloch states.

B. Heisenberg picture

At times $t > t_{\text{initial}}$ we now specialize to a constant field and set

$$\mathbf{K}(t) = \frac{e}{\hbar} \mathbf{E}_{\text{dc}} t. \quad (21)$$

To make $\mathbf{K}(t)$ continuous as the field is turned on, we take

$$\mathbf{K}^o = \frac{e}{\hbar} \mathbf{E}_{\text{dc}} t_{\text{initial}}. \quad (22)$$

We move into the Heisenberg picture, which is only slightly more complicated than usual because the Hamiltonian has an explicit time dependence. We begin by introducing an evolution operator $\hat{U}(t)$ satisfying

$$i\hbar \frac{d\hat{U}(t)}{dt} = H(t) \hat{U}(t) \quad (23)$$

and, for definitiveness, the condition $\hat{U}(t = t_{\text{initial}}) = 1$. The Schrödinger picture ket evolves, then, according to $|\Psi^S(t)\rangle = \hat{U}(t) |\Psi^H\rangle$, where we have put $|\Psi^H\rangle \equiv |\Psi^S(t = t_{\text{initial}})\rangle$, and the

expectation value of any Schrödinger operator \mathcal{O} at time t is given by $\langle \Psi^S(t) | \mathcal{O} | \Psi^S(t) \rangle = \langle \Psi^H | \mathcal{O}^H(t) | \Psi^H \rangle$, where the corresponding Heisenberg operator $\mathcal{O}^H(t) = \hat{U}^\dagger(t) \mathcal{O} \hat{U}(t)$. Using Eq. (23) it is easy to demonstrate that

$$i\hbar \frac{d\mathcal{O}^H(t)}{dt} = [\mathcal{O}^H(t), H^H(t)], \quad (24)$$

where

$$H^H(t) = \hat{U}^\dagger(t) H(t) \hat{U}(t) = \int [\psi^H(\mathbf{x}, t)]^\dagger \mathcal{H}(t) \psi^H(\mathbf{x}, t) d\mathbf{x}, \quad (25)$$

where we have used Eq. (1), and $\mathcal{H}(t)$, which contains no operators, is unchanged.

We use the time-dependent basis functions $\{\bar{\chi}_m(\mathbf{k}; \mathbf{x})\}$ to expand $\psi^H(\mathbf{x}, t)$

$$\psi^H(\mathbf{x}, t) = \sum_{nk} b_{nk}(t) \bar{\chi}_n(\mathbf{k}; \mathbf{x}), \quad (26)$$

where

$$b_{nk}(t) = \int \bar{\chi}_n^*(\mathbf{k}; \mathbf{x}) \psi^H(\mathbf{x}, t) d\mathbf{x}. \quad (27)$$

Since the basis is complete we find $\{b_{nk}(t), b_{mk}^\dagger(t)\} = \delta_{nm} \delta_{\mathbf{k}\mathbf{k}'}$, which follows using the anticommutation relations given in Eq. (3) and the fact that equal time versions of these are preserved in the Heisenberg picture.

There is no superscript H over $b_{nk}(t)$ because it is not a “pure” Heisenberg operator in the sense of satisfying Eq. (24). While $\psi^H(\mathbf{x}, t)$ is such an operator, the fact that $\bar{\chi}_n^*(\mathbf{k}; \mathbf{x})$ contains an explicit time dependence means that there is an extra term in the dynamics for $b_{nk}(t)$, which is discussed in detail in Appendix A. Even before that is done, we are in a position to identify the time-independent Heisenberg ket $|\Psi^H\rangle$, which corresponds to the Schrödinger ket at $t=t_{\text{initial}}$. We see from Eq. (26) that we have

$$\psi^H(\mathbf{x}, t) = \sum_{nk} b_{nk}(t) \bar{\phi}_n(\mathbf{k}; \mathbf{x}) e^{-i\omega_n(\mathbf{k}+\mathbf{K}^o)t}$$

for $t < t_{\text{initial}}$, where we have used Eq. (20). From Eq. (9) and the equality of $\bar{\phi}_n(\mathbf{k}; \mathbf{x})$ and $\phi_n(\mathbf{k}+\mathbf{K}_o; \mathbf{x})$ for $t < t_{\text{initial}}$ we see that all the time dependence required of $\psi^H(\mathbf{x}, t)$ by the Hamiltonian at these early times resides in the time-dependent phase factors. Hence at such times $b_{nk}(t)$ is in fact time-independent; we write it as b_{nk} , so for $t < t_{\text{initial}}$, $b_{nk}(t) = b_{nk}$, and

$$\psi^H(\mathbf{x}, t < t_{\text{initial}}) = \sum_{nk} b_{nk} \bar{\phi}_n(\mathbf{k}; \mathbf{x}) e^{-i\omega_n(\mathbf{k}+\mathbf{K}^o)t}. \quad (28)$$

Clearly b_{nk} is the destruction operator associated with an electron with band index n and crystal momentum $\mathbf{k}+\mathbf{K}^o$. Now our ket $|\Psi^H\rangle$ should describe the “semiconductor vacuum,” in which the valence bands are completely filled and the conduction bands completely empty. So it must be possible to divide the bands into a set of conduction bands (c) and a set of valence bands (v) for which

$$b_{c\mathbf{k}} |\Psi^H\rangle = 0, \quad (29)$$

$$b_{v\mathbf{k}}^\dagger |\Psi^H\rangle = 0 \quad (30)$$

for all \mathbf{k} in the first Brillouin zone.

C. Interaction picture

We now move into an interaction picture, where the time independent ket $|\Psi^H\rangle$ is replaced by a time dependent ket $|\Psi(t)\rangle$ that evolves according to the interaction Hamiltonian $H_{\text{eff}}(t)$

$$i\hbar \frac{d|\Psi(t)\rangle}{dt} = H_{\text{eff}}(t) |\Psi(t)\rangle, \quad (31)$$

where $H_{\text{eff}}(t)$ describes the effect of the optical field in the presence of the dc field. In Appendix A we show that it is given by

$$H_{\text{eff}}(t) = -\frac{1}{c} \mathbf{A}_{\text{opt}}(t) \cdot \tilde{\mathcal{J}}(t), \quad (32)$$

where

$$\tilde{\mathcal{J}}(t) = e \sum_{n_1, n_2, \mathbf{k}} b_{n_2, \mathbf{k}}^\dagger b_{n_1, \mathbf{k}} \tilde{\mathbf{V}}_{n_2 n_1}(\mathbf{k}; t) \quad (33)$$

with

$$\tilde{\mathbf{V}}_{nq}(\mathbf{k}; t) = \sum_{m,p} L_{mn}^*(\mathbf{k}; t) \mathbf{V}_{mp}(\mathbf{k}; t) L_{pq}(\mathbf{k}; t). \quad (34)$$

The evolution matrix $L(\mathbf{k}; t)$ is chosen so that it satisfies

$$i\hbar \frac{dL(\mathbf{k}; t)}{dt} = [T(\mathbf{k}; t) + S(\mathbf{k}; t)] L(\mathbf{k}; t), \quad (35)$$

where

$$T_{pm}(\mathbf{k}; t) = \delta_{pm} \hbar \omega_m [\mathbf{k} + \mathbf{K}(t)],$$

$$S_{pm}(\mathbf{k}; t) = -\boldsymbol{\mu}_{pm}(\mathbf{k}; t) \cdot \mathbf{E}_{\text{dc}}(t). \quad (36)$$

Since $H_{\text{eff}}(t)$ vanishes for $t < t_{\text{initial}}$, before the optical field is applied, we can take the initial condition of this differential equation to be $|\Psi(-\infty)\rangle = |\Psi^H\rangle$. The matrix elements $\mathbf{V}_{mp}(\mathbf{k}; t)$ describe the coupling between bands by the optical field, in the presence of the dc field; the matrix elements $\tilde{\mathbf{V}}_{nq}(\mathbf{k}; t)$ appearing in $H_{\text{eff}}(t)$ are effective matrix elements that take into account the fact that the dc field can induce transitions between these bands itself.

D. Perturbation calculation

With the interaction picture in hand we can now calculate the effect of optical transitions on the populations of the different bands. The usual iterative solution of the Schrödinger equation [Eq. (31)] is

$$|\Psi(t)\rangle = |\Psi^H\rangle + |\Psi^{(1)}(t)\rangle + \dots, \quad (37)$$

where to first order we find

$$|\Psi^{(1)}\rangle = \frac{1}{i\hbar} \int_{-\infty}^{\infty} H_{\text{eff}}(t') |\Psi^H\rangle dt' \quad (38)$$

taking $|\Psi^{(1)}\rangle$ to denote the value of $|\Psi^{(1)}(t)\rangle$ at times after the optical pulse has passed. We are interested in calculating the number of electrons in the conduction bands. The conduction band number operator is

$$N_c \equiv \sum_{\mathbf{c}\mathbf{k}} b_{\mathbf{c}\mathbf{k}}^\dagger b_{\mathbf{c}\mathbf{k}} \quad (39)$$

and the expectation value is $\mathcal{N}_c(t) = \langle \Psi(t) | N_c | \Psi(t) \rangle$. We denote by $|\Psi\rangle$ the value of $|\Psi(t)\rangle$ at times after the optical pulse has passed; it is clear from Eqs. (31) and (32) that at these times the ket is no longer changing in time. At such times we have, as shown in Appendix A

$$\mathcal{N}_c(t) = \sum_{c,n,m,\mathbf{k}} L_{nc}^*(\mathbf{k};t) L_{mc}(\mathbf{k};t) \langle \Psi | b_{n\mathbf{k}}^\dagger b_{m\mathbf{k}} | \Psi \rangle. \quad (40)$$

E. Simplifications

In our calculations we choose the $\hat{\mathbf{z}}$ direction as that in which the dc field points, putting $\mathbf{E}_{\text{dc}} = E_{\text{dc}} \hat{\mathbf{z}}$ in Eq. (21), and defining a normalized electric field amplitude

$$\varepsilon \equiv \frac{eE_{\text{dc}}}{\hbar}. \quad (41)$$

With the special role the $\hat{\mathbf{z}}$ direction plays, it is useful to decompose each \mathbf{k} according to $\mathbf{k} = \mathbf{k}_\perp + k_\parallel \hat{\mathbf{z}}$, where \mathbf{k}_\perp lies in the (k_x, k_y) plane. We exhibit the \mathbf{k}_\perp and k_\parallel components explicitly by writing $\mathbf{V}_{mp}(\mathbf{k};t)$ as $\mathbf{V}_{mp}(\mathbf{k}_\perp, k_\parallel; t)$, and similarly for all quantities dependent on \mathbf{k} .

To specify any such quantity one might think that a separate function of time would be required for each \mathbf{k} in the Brillouin zone but once the dc field has been on for a long enough time that is not true. Because the evolution of $\mathbf{K}(t)$ drives the instantaneous wave vector of the Bloch state through the Brillouin zone [see Eq. (9) and the discussion leading to Eq. (13)], the time dependence of functions like $\mathbf{V}_{mp}(\mathbf{k}_\perp, k_\parallel; t)$ is mirrored by their dependence on k_\parallel . In Appendix B we show that

$$\mathbf{V}_{mn}(\mathbf{k}_\perp, k_\parallel; t) = e^{-i\sigma_{mn}(\mathbf{k}_\perp, k_\parallel)} \mathbf{V}_{mn}\left(\mathbf{k}_\perp, 0; t + \frac{k_\parallel}{\varepsilon}\right), \quad (42)$$

where

$$\sigma_{mn}(\mathbf{k}_\perp, k_\parallel) \equiv -\varepsilon \int_{-k_\parallel/\varepsilon}^0 [\xi_{mn}^z(\mathbf{k}_\perp + k_\parallel \hat{\mathbf{z}} + \varepsilon t' \hat{\mathbf{z}}) - \xi_{mn}^z(\mathbf{k}_\perp + k_\parallel \hat{\mathbf{z}} + \varepsilon t' \hat{\mathbf{z}})] dt' \quad (43)$$

is independent of time although it does depend on the dc electric field strength. Corresponding results hold for $S_{pm}(\mathbf{k}_\perp, k_\parallel; t)$ and $T_{pm}(\mathbf{k}_\perp, k_\parallel; t)$. From these results it follows, as we show in Appendix B, that

$$\hat{L}_{pn}(\mathbf{k}_\perp, k_\parallel; t) = \sum_q m_{pq} \left(\mathbf{k}_\perp; t + \frac{k_\parallel}{\varepsilon} \right) \mathcal{B}_{qn}(\mathbf{k}_\perp, k_\parallel), \quad (44)$$

where we have put

$$\hat{L}_{pn}(\mathbf{k}_\perp, k_\parallel; t) \equiv L_{pn}(\mathbf{k}_\perp, k_\parallel; t) e^{i\sigma_{pn}(\mathbf{k}_\perp, k_\parallel)} \quad (45)$$

and the matrix $m_{pn}(\mathbf{k}_\perp; t)$ satisfies

$$i\hbar \frac{dm_{pn}(\mathbf{k}_\perp; t)}{dt} = \sum_q [T_{pq}(\mathbf{k}_\perp, 0; t) + S_{pq}(\mathbf{k}_\perp, 0; t)] m_{qn}(\mathbf{k}_\perp; t) \quad (46)$$

together with the initial condition

$$m_{pn}(\mathbf{k}_\perp; 0) = \delta_{pn}. \quad (47)$$

The matrix elements $\mathcal{B}_{qn}(\mathbf{k}_\perp, k_\parallel)$ encode the initial conditions of the $L_{pn}(\mathbf{k}_\perp, k_\parallel; t)$; in the dynamics of the $L_{pn}(\mathbf{k}_\perp, k_\parallel; t)$ we see from Eq. (44) that, like the dynamics of $\mathbf{V}_{mn}(\mathbf{k}_\perp, k_\parallel; t)$, there is a mirroring of the dependence on t with that on k_\parallel . This mirroring will greatly simplify the calculations below. But before we turn to them, we must address a crucial approximation.

F. Block diagonal approximation

When the dc field turns on at t_{initial} , long before the optical pulse arrives, there will be an onset of Zener tunneling between the valence and conduction bands that will build up as time goes on. In an actual experiment, of course, a steady state will be set up determined by various relaxation mechanisms. These are not included in our formalism. Hence, it would be unrealistic to try to imagine allowing the dc field to be on for an infinite amount of time before the optical pulse arrives. As well, it would be unphysical to miscount the Zener tunneling that would continue after the pulse has passed as being associated with absorption. In the kind of independent particle approximation we are employing here, the best we can do is to use as an input to our description the fact that we expect the Zener tunneling across the band gap to be small, and neglect it.

The neglect of valence band to conduction band Zener tunneling corresponds to the neglect of the matrix elements $S_{qn}(\mathbf{k}_\perp, k_\parallel; t)$ in Eq. (35) that involve one of (q, n) being a conduction band and the other a valence band. With this approximation Eq. (35) for $L(\mathbf{k}_\perp, k_\parallel; t)$ splits into two matrix equations, one for the conduction bands and one for the valence bands. Similarly, of course, Eq. (46) for $m(\mathbf{k}_\perp; t)$ splits into two blocks as well.

Equation (44) then can be written in terms of the two sub-blocks

$$\hat{L}_{cc'}(\mathbf{k}_\perp, k_\parallel; t) = \sum_{c''} m_{cc''} \left(\mathbf{k}_\perp; t + \frac{k_\parallel}{\varepsilon} \right) \mathcal{B}_{c''c'}(\mathbf{k}_\perp, k_\parallel),$$

$$\hat{L}_{vv'}(\mathbf{k}_\perp, k_\parallel; t) = \sum_{v''} m_{vv''} \left(\mathbf{k}_\perp; t + \frac{k_\parallel}{\varepsilon} \right) \mathcal{B}_{v''v'}(\mathbf{k}_\perp, k_\parallel), \quad (48)$$

where (c, v) [and (c', v') , etc.] refer to conduction and valence bands. Note that $\mathcal{B}_{c''c'}(\mathbf{k}_\perp, k_\parallel)$ and $\mathcal{B}_{v''v'}(\mathbf{k}_\perp, k_\parallel)$ are elements of unitary matrices, since by Eq. (47) they specify the values of $\hat{L}_{cc'}(\mathbf{k}_\perp, k_\parallel; -k_\parallel/\varepsilon)$ and $\hat{L}_{vv'}(\mathbf{k}_\perp, k_\parallel; -k_\parallel/\varepsilon)$; by construction the $L(\mathbf{k}_\perp, k_\parallel; t)$ are unitary matrices, and it is easy to

confirm that the $\hat{L}(\mathbf{k}_\perp, k_\parallel; t)$ [Eq. (45)] are as well. The actual values of $\mathcal{B}_{c'c'}(\mathbf{k}_\perp, k_\parallel)$ and $\mathcal{B}_{v'v'}(\mathbf{k}_\perp, k_\parallel)$ will turn out to be unimportant.

The ‘‘block approximation’’ [Eq. (48)] will be employed hereafter. Whenever we denote general indices (such as n and q) for matrix components, as we do below, we understand that they are either both conduction band indices or both valence band indices. The approximation has important consequences for calculating the total number of electrons $\mathcal{N}_c(t)$ promoted to the conduction bands after the pulse has passed. In Appendix B, it is shown that, when this approximation is made, Eq. (40) reduces to

$$\mathcal{N}_c(t) = \sum_{c', \mathbf{k}_\perp, k_\parallel} \langle \Psi | b_{c' \mathbf{k}_\perp, k_\parallel}^\dagger b_{c' \mathbf{k}_\perp, k_\parallel} | \Psi \rangle \quad (49)$$

for $t > t_{\text{end}}$. The fact that \mathcal{N}_c is a constant after the optical pulse has passed reflects the fact that we have neglected Zener tunneling between valence and conduction bands.

G. Linear absorption in the presence of a dc field

Equations (42) and (48) allow us to write a simplified expression for $\tilde{V}_{nq}(\mathbf{k}; t)$ in Eq. (34), which when used in the expression for $H_{\text{eff}}(t)$ [Eqs. (32) and (33)] allows us to calculate $|\Psi^{(1)}\rangle$ according to Eq. (38)

$$|\Psi^{(1)}\rangle = \sum_{\mathbf{k}_\perp, k_\parallel} \sum_{v, c} \int d\omega \theta_{cv\mathbf{k}_\perp}^j(\omega) E^i(\omega) e^{i\omega k_\parallel/\varepsilon} \overline{|cv(\mathbf{k}_\perp, k_\parallel)\rangle}, \quad (50)$$

where

$$\theta_{cv\mathbf{k}_\perp}^j(\omega) = \frac{e}{2\pi\hbar} \frac{F_{cv}^j(\mathbf{k}_\perp; -\omega)}{\omega} \quad (51)$$

and

$$\mathbf{F}_{cv}(\mathbf{k}_\perp; -\omega) \equiv \int_{-\infty}^{\infty} \mathbf{F}_{cv}(\mathbf{k}_\perp; t) e^{-i\omega t} dt \quad (52)$$

with

$$\mathbf{F}_{cv}(\mathbf{k}_\perp; t) = \sum_{c', v'} m_{c'c}^*(\mathbf{k}_\perp; t) \mathbf{V}_{c'v'}(\mathbf{k}_\perp, 0; t) m_{v'v}(\mathbf{k}_\perp; t) \quad (53)$$

and where $\mathbf{E}(\omega)$ is the Fourier transform of our optical field

$$\mathbf{E}_{\text{opt}}(t) = \int \frac{d\omega}{2\pi} \mathbf{E}(\omega) e^{-i\omega t}. \quad (54)$$

The details are given in Appendix C. The state $\overline{|cv(\mathbf{k}_\perp, k_\parallel)\rangle}$ corresponds to one electron removed from the valence bands and one deposited in the conduction bands, as described in that appendix; these states satisfy

$$\overline{\langle c'v'(\mathbf{k}'_\perp, k'_\parallel) | cv(\mathbf{k}_\perp, k_\parallel) \rangle} = \delta_{c'c} \delta_{v'v} \delta_{\mathbf{k}'_\perp \mathbf{k}_\perp} \delta_{k'_\parallel k_\parallel} \quad (55)$$

and $|\Psi^{(1)}\rangle$, consisting of a superposition of these states, is an eigenstate of the number operator for electrons in the con-

duction bands, with eigenvalue unity. Thus to lowest order the expectation value of the number of electrons in the conduction bands [Eq. (49)] is simply given by

$$\mathcal{N}_c = \langle \Psi^{(1)} | \Psi^{(1)} \rangle \quad (56)$$

or

$$\begin{aligned} \mathcal{N}_c &= \sum_{\mathbf{k}_\perp, k_\parallel} \sum_{v, c} \int \int d\omega d\omega' \theta_{cv\mathbf{k}_\perp}^j(\omega) [\theta_{cv\mathbf{k}_\perp}^j(\omega')]^* \\ &\quad \times e^{i(\omega-\omega')k_\parallel/\varepsilon} E^i(\omega) [E^j(\omega')]^*. \end{aligned} \quad (57)$$

Converting the sum over \mathbf{k}_\perp and k_\parallel to integrals, we have

$$\begin{aligned} n &= \int \int d\omega d\omega' \\ &\quad \times \left\{ \sum_{v, c} \int \int \frac{d\mathbf{k}_\perp}{4\pi^2} \frac{dk_\parallel}{2\pi} \theta_{cv\mathbf{k}_\perp}^j(\omega) [\theta_{cv\mathbf{k}_\perp}^j(\omega')]^* e^{i(\omega-\omega')k_\parallel/\varepsilon} \right\} \\ &\quad \times E^i(\omega) [E^j(\omega')]^*, \end{aligned}$$

where $n = \mathcal{N}_c / \Omega$, where Ω is the integration volume. Now we take

$$\int \frac{dk_\parallel}{2\pi} e^{i(\omega-\omega')k_\parallel/\varepsilon} = \delta\left(\frac{\omega-\omega'}{\varepsilon}\right) = |\varepsilon| \delta(\omega-\omega') \quad (58)$$

for a small enough electric field and we then have

$$\begin{aligned} n &= \int_0^\infty d\omega \left\{ |\varepsilon| \sum_{v, c} \int \int \frac{d\mathbf{k}_\perp}{4\pi^2} \theta_{cv\mathbf{k}_\perp}^j(\omega) [\theta_{cv\mathbf{k}_\perp}^j(\omega)]^* \right\} \\ &\quad \times E^i(\omega) [E^j(\omega)]^*. \end{aligned}$$

We have restricted the integral over ω to positive frequencies. In the absence of a dc field, there would only be absorption for $\omega > \omega_{cv}(\mathbf{k})$. Here it will acquire some strength even below the gap but for sufficiently small fields there is no problem in limiting the integral to positive frequencies.

Equation (58) is appropriate for a pulse; to go to the continuous wave limit, we take the limit to a long pulse in the usual way. Writing

$$\mathbf{E}_{\text{opt}}(t) = \mathbf{E}_o e^{-i\omega_o t} + \mathbf{E}_o^* e^{i\omega_o t}$$

for $-T/2 < t < T/2$ and vanishing otherwise, taking the Fourier transform [Eq. (54)] we find

$$E^i(\omega) [E^j(\omega)]^* \rightarrow E_o^i (E_o^j)^* \left[\frac{\sin \frac{1}{2}(\omega - \omega_o)T}{\frac{1}{2}(\omega - \omega_o)T} \right]^2$$

for $\omega > 0$ and $\omega_o T \gg 1$. Assuming then that $1/T$ is smaller than the range over which the term multiplying $E^i(\omega) [E^j(\omega)]^*$ in the integrand of Eq. (58) varies significantly, we can take

$$E^i(\omega) [E^j(\omega)]^* \rightarrow 2\pi T E_o^i (E_o^j)^* \delta(\omega - \omega_o)$$

in Eq. (58) and, identifying n/T with dn/dt , we have the Fermi's golden rule limit

$$\frac{dn}{dt} = 2\pi \left\{ |\varepsilon| \sum_{v,c} \int \int \frac{d\mathbf{k}_\perp}{4\pi^2} \theta_{cv\mathbf{k}_\perp}^j(\omega_o) [\theta_{cv\mathbf{k}_\perp}^j(\omega_o)]^* \right\} E_o^i (E_o^j)^*. \quad (59)$$

In Appendix D, the analogous expression is found for no dc field. It is

$$\frac{dn}{dt} = 2\pi \left\{ \int \frac{d\mathbf{k}}{8\pi^3} \sum_{cv} \gamma_{cv\mathbf{k}}^j (\gamma_{cv\mathbf{k}}^j)^* \delta[\omega_o - \omega_{cv}(\mathbf{k})] \right\} E_o^i (E_o^j)^*, \quad (60)$$

where

$$\gamma_{cv\mathbf{k}}^j = \frac{e v_{cv}^i(\mathbf{k})}{\hbar \omega_{cv}(\mathbf{k})}. \quad (61)$$

Equations (59) and (60) are of the form

$$\frac{dn}{dt} = \eta^{ij}(\omega_o) E_o^i (E_o^j)^*, \quad (62)$$

where $\eta^{ij}(\omega)$ is a tensor that describes the polarization-dependent optical carrier injection rate. To relate this to the absorption spectrum $\alpha(\omega)$, we identify $\text{Im}[\varepsilon^{ij}(\omega)] = 2\pi\hbar \eta^{ij}(\omega)$, where the $\varepsilon^{ij}(\omega)$ are the elements of the dielectric tensor. Assuming that the dc field points along one of the principal axes of the dielectric tensor, we can use the expression²⁰

$$\alpha(\omega) = \frac{\text{Im}[\varepsilon^{ii}(\omega)]\omega}{n(\omega)c} = \frac{2\pi\hbar\omega\eta^{ii}(\omega)}{n(\omega)c}, \quad (63)$$

(no summation implied) where i is the direction of polarization of the optical field, assumed to be linearly polarized along one of the principal axes, and $n(\omega)$ is the refractive index associated with the propagation of light with this polarization. In principle $n(\omega)$ is modified by the presence of a dc field since through Kramers-Kronig relations $n(\omega)$ can be written in terms of an integral involving $\eta^{ij}(\omega)$ at all frequencies. But in GaAs, the material we consider in presenting our sample calculations, even near the band gap the relative change in $n(\omega)$ due to the presence of a dc field is much less than the relative change of $\eta^{ij}(\omega)$ so in Eq. (63) we always take $n(\omega)$ as the appropriate refractive index in the absence of a dc field. The dielectric tensor is proportional to the unit tensor in the absence of an electric field for GaAs and thus any direction of an applied dc field can be taken to identify one of the principal axes.

In Appendix E, it is shown that for two parabolic bands and constant matrix elements V_{cv} , our theory reproduces the well-known Airy function expression³

$$\alpha(\omega) = \frac{2\pi e^2 \mu_{cv} \varepsilon}{\hbar^2 \omega \Omega_{cv} n(\omega) c} |V_{cv}|^2 \times \left\{ -\frac{\omega_g - \omega}{\Omega_{cv}} \text{Ai}^2\left(\frac{\omega_g - \omega}{\Omega_{cv}}\right) + \left[\text{Ai}'\left(\frac{\omega_g - \omega}{\Omega_{cv}}\right) \right]^2 \right\}, \quad (64)$$

where $\hbar\omega_g$ is the band gap energy and $\Omega_{cv} \equiv (\hbar\varepsilon^2/2\mu_{cv})^{1/3}$ is the electro-optic frequency, where μ_{cv} is the reduced mass.

Overall, our general expression Eq. (59) for the absorption in an electric field contains one less integral than those derived by Enderlein, Renner, and Scheele¹² and by Aspnes, Handler, and Blossey.²¹ Hader, Linder, and Döhler found a similar simplification in their theory.⁸ It is the linear relationship between t and k_\parallel for a dc field that enables the removal of one of the integrals. The integral over k_\parallel is converted into a Fourier transform and we integrate over \mathbf{k}_\perp rather than the entire Brillouin zone (BZ). As discussed in more detail in the next section, we interpret this as a sum over all possible trajectories carriers can take through reciprocal space. The absorption spectrum for each trajectory, for a given pair of bands and i -polarized light, is proportional to $|\theta_{cv\mathbf{k}_\perp}^j(\omega)|^2$.

III. CALCULATIONS

For an example calculation, we use a $\mathbf{k} \cdot \mathbf{p}$ model¹⁸ for the band structure, in which known band energies and matrix elements at the Γ point are used to calculate the band dispersion and the variation in the matrix elements with \mathbf{k} . For a Hamiltonian \mathcal{H}_0 , a $\mathbf{k} \cdot \mathbf{p}$ Hamiltonian

$$H_{\mathbf{k}} = e^{-i\mathbf{k} \cdot \mathbf{r}} \mathcal{H}_0 e^{i\mathbf{k} \cdot \mathbf{r}} = \mathcal{H}_0 + \frac{\hbar^2 k^2}{2m} + \hbar \mathbf{k} \cdot \mathbf{v} \quad (65)$$

can be defined for the u functions, so that $H_{\mathbf{k}} u_n(\mathbf{k}; \mathbf{x}) = \hbar\omega_n(\mathbf{k}) u_n(\mathbf{k}; \mathbf{x})$, recalling $\phi_n(\mathbf{k}; \mathbf{x}) = \Omega^{-1/2} u_n(\mathbf{k}; \mathbf{x}) e^{i\mathbf{k} \cdot \mathbf{x}}$. Since $\{\phi_n(\mathbf{k}=\mathbf{0}; \mathbf{x})\}$ form a complete set of states with the periodicity of the lattice, one could, in principle, calculate the full band structure by moving from the center of the Brillouin zone to any other point with successive applications of Eq. (65), as long as the energies $\hbar\omega_n$ and matrix elements \mathbf{v}_{mn} at the center of the Brillouin zone are known. In practical models, the set of bands is truncated to a manageable number. Important effects from bands outside the set can be taken into account using \mathbf{k} -dependent remote band parameters in an extra term $H^R(\mathbf{k})$ so that

$$(H_{\mathbf{k}})_{mn} = (H_0)_{mn} + \frac{\hbar^2 k^2}{2m} \delta_{mn} + \hbar \mathbf{k} \cdot \mathbf{v}_{mn} + [H^R(\mathbf{k})]_{mn}, \quad (66)$$

where H_0 contains the band energies at $\mathbf{k}=\mathbf{0}$ and off-diagonal terms due to spin-orbit coupling.²²

Calculations of the FKE have been done previously using empirical models for the band structure. Enderlein *et al.*¹² used a Kohn-Luttinger model for the valence bands. Hader *et al.*⁸ used a Kane model that includes the valence bands and the lowest energy conduction bands. Here we use a model that directly includes 14 bands and includes effects from bands outside that set to order k^2 .²³ Fourteen-band models²⁴ (also known as five-level models) have been previously applied to calculations of band structure^{23,25-28} and linear optical properties^{29,30} of semiconductors. To examine the effects of band structure on the FKE, we also calculate using four submodels derived from the 14-band model.

A. Band structure models

The 14-band model used²³ directly includes three groups of bands: six p -like valence bands, the two lowest in energy

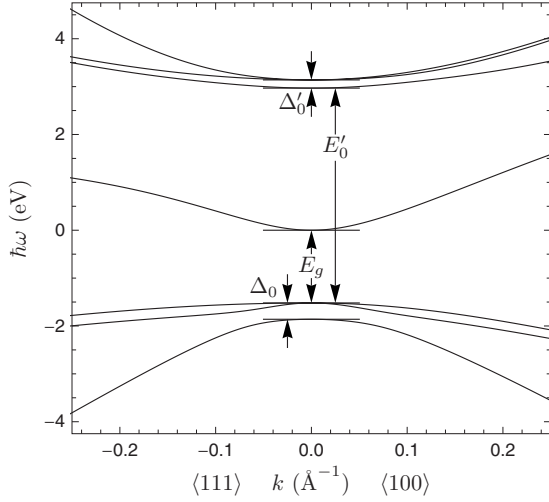


FIG. 1. Bands calculated using from the H_{14} model along two directions in the BZ. The energy splittings at $\mathbf{k}=0$ defined in the model are labeled. Spin splitting is not shown.

s -like conduction bands, and the six next higher in energy p -like conduction bands. For the model parameters, we use the notation of Bhat and Sipe,³¹ denoting the fundamental band gap E_g , the valence band spin-orbit energy Δ_0 , the valence band to upper conduction band energy E'_0 , and the upper conduction band spin-orbit energy Δ'_0 . The valence to conduction band spin-orbit coupling,²² which contributes to off-diagonal terms in H_0 , is denoted Δ^- . The model contains three coupling parameters: P_0 between the valence and conduction bands, Q between the valence and upper conduction bands, and P'_0 between the lowest conduction band and upper conduction bands. The bands considered in the model are shown in Fig. 1.

The model also includes the effects of remote bands through Löwdin perturbation theory.³² The remote band parameters include modified Luttinger parameters γ_1 , γ_2 , and γ_3 and a parameter F that fixes the curvature of the lowest conduction band to the experimentally determined effective mass. The modified Luttinger parameters are related to the usual Luttinger parameters γ_{1L} , γ_{2L} , and γ_{3L} by

$$\gamma_1 = \gamma_{1L} - \frac{E_P}{3E_g} - \frac{E_Q}{3E'_0} - \frac{E_Q}{3(E'_0 + \Delta'_0)},$$

TABLE I. Model parameters for GaAs. The coupling parameters P'_0 and Q are given in units of eV \AA , the spin splitting Δ^- is given in eV, and the k -linear term C_k is given in meV \AA . The Γ -point energy splittings and the coupling between the valence bands and lower conduction bands are the same for all models: $E_g = 1.519$ eV, $\Delta_0 = 0.341$ eV, $E'_0 = 4.488$ eV, $\Delta'_0 = 0.171$ eV, and $P_0 = 10.3$ eV \AA .

Model	γ_1	γ_2	γ_3	F	P'_0	Q	Δ^-	C_k
H_{14}	-0.581	-0.019	-0.333	1.055	3.0	7.7	-0.061	-3.4
H_{14NS}	-0.581	-0.019	-0.333	1.055	3.0	7.7	0	0
H_{14NR}	-1	0	0	0	3.0	7.7	0	0
H_8	1.687	-0.597	0.244	1.055	0	0	0	0
H_{8S}	1.687	-0.092	-0.092	1.055	0	0	0	0

$$\gamma_2 = \gamma_{2L} - \frac{E_P}{6E_g} + \frac{E_Q}{6E'_0},$$

$$\gamma_3 = \gamma_{3L} - \frac{E_P}{6E_g} - \frac{E_Q}{6E'_0}, \quad (67)$$

where $E_P = 2mP_0^2/\hbar^2$ and $E_Q = 2mQ^2/\hbar^2$. The model also includes a remote band parameter C_k that adds a small k -linear term to the valence bands.³³ We refer the reader to the work of Pfeffer and Zawadzki,²³ and Bhat and Sipe³¹ for details of the model, including the basis states and the 14×14 $H_{\mathbf{k}}$ matrix.

We calculate spectra here for GaAs, using $\gamma_{1L} = 7.797$, $\gamma_{2L} = 2.458$, and $\gamma_{3L} = 3.299$. We performed the calculations using the full 14-band model, denoted H_{14} , and four other models derived from it. To examine the effects of the k -linear remote band terms and the interband spin-orbit coupling in the calculation, we define a “no spin” model H_{14NS} in which we have set $\Delta^- = 0$ and $C_k = 0$. We use a bare 14-band model to examine the effects of remote band parameters. In that model, denoted H_{14NR} , we set all remote band parameters and Δ^- equal to zero. Thus, effective masses calculated from H_{14NR} do not match experimentally observed values but critical point energies and the symmetry of the matrix elements are maintained. For direct comparison with the previous work of Hader *et al.*,⁸ we have implemented an eight-band model, denoted H_8 , by setting $P'_0 = Q = 0$ in the 14-band model and renormalizing the modified Luttinger parameters according to Eq. (67). Finally, to examine the effects of band warping, we use a spherical eight-band model, denoted H_{8S} , in which both γ_{2L} and γ_{3L} are set equal to $(2\gamma_{2L} + 3\gamma_{3L})/5 = 2.963$.³⁴ The parameters for each model are given in Table I.

B. Matrix elements

Time-dependent velocity matrix elements $\mathbf{V}_{mn}(\mathbf{k}_\perp; t)$ enter the calculation through Eqs. (53) and (36) [in the latter equation through $\boldsymbol{\mu}_{mn}(\mathbf{k}_\perp; t)$, defined in Eq. (12)]. In a typical $\mathbf{k} \cdot \mathbf{p}$ calculation of optical absorption,²⁹ matrix elements are found by diagonalizing $H_{\mathbf{k}}$ at each \mathbf{k} and using the resulting eigenvectors to project the velocity matrix elements at $\mathbf{k}=0$ into the new basis. The FKE, however, depends on the magnitude and the relative phase of the matrix elements along a trajectory in the BZ, so diagonalization, which introduces random phases, does not work.

We decompose the time-dependent \bar{u} functions [see discussion after Eq. (12)] into linear combinations of the time-independent u functions at $\mathbf{k}=\mathbf{0}$

$$\bar{u}_n(\mathbf{k}_\perp; \mathbf{x}) = \sum_m C_{mn}(\mathbf{k}_\perp; t) u_m(\mathbf{0}; \mathbf{x}). \quad (68)$$

Multiplying by $u_m^*(\mathbf{0}; \mathbf{x})$, integrating over the unit cell, and using

$$\frac{1}{V} \int u_m^*(\mathbf{0}; \mathbf{x}) u_m(\mathbf{0}; \mathbf{x}) d\mathbf{x} = \delta_{m'm}, \quad (69)$$

where V is the unit cell volume, we have

$$C_{mn}(\mathbf{k}_\perp; t) = \frac{1}{V} \int u_m^*(\mathbf{0}; \mathbf{x}) \bar{u}_n(\mathbf{k}_\perp; \mathbf{x}) d\mathbf{x}. \quad (70)$$

The time dependence of $C_{mn}(\mathbf{k}_\perp; t)$ arises from the implicit time dependence of $\bar{u}_n(\mathbf{k}_\perp; \mathbf{x})$. From Eqs. (11) and (12), using our assumed dc field, we have

$$\frac{d\bar{u}_n(\mathbf{k}_\perp; \mathbf{x})}{dt} = -\varepsilon \sum_{q \neq n} \bar{u}_q(\mathbf{k}_\perp; \mathbf{x}) \frac{V_{qn}^z(\mathbf{k}_\perp; t)}{\omega_{qn}(\mathbf{k}_\perp + \varepsilon t \hat{\mathbf{z}})}, \quad (71)$$

where we have used the assumption that ε is independent of time. Using Eq. (70), this leads to

$$\frac{dC_{mn}(\mathbf{k}_\perp; t)}{dt} = -\varepsilon \sum_{q \neq n} C_{mq}(\mathbf{k}_\perp; t) \frac{V_{qn}^z(\mathbf{k}_\perp; t)}{\omega_{qn}(\mathbf{k}_\perp + \varepsilon t \hat{\mathbf{z}})}. \quad (72)$$

At $t=0$, $\bar{u}_n(\mathbf{k}; \mathbf{x}) = u_n(\mathbf{k}; \mathbf{x})$ so the initial condition $C_{mn}(\mathbf{k}_\perp; 0)$ can be found by diagonalizing $H_{\mathbf{k}}$ at $\mathbf{k}=\mathbf{k}_\perp$. What is needed to solve Eq. (72) is to evaluate $V_{qn}^z(\mathbf{k}_\perp; t)$ at each step.

From Eq. (10), with our assumed field, we have

$$\mathbf{V}_{mn}(\mathbf{k}_\perp; t) = \frac{1}{m} \int \bar{\phi}_m^*(\mathbf{k}_\perp; \mathbf{x}) \left(\frac{\hbar}{i} \nabla + \hbar \varepsilon t \hat{\mathbf{z}} \right) \bar{\phi}_n(\mathbf{k}_\perp; \mathbf{x}) d\mathbf{x}. \quad (73)$$

Expressing this in terms of the \bar{u} functions and using Eq. (68), it can be shown that the matrix elements are given in terms of $C_{mn}(\mathbf{k}_\perp; t)$ by

$$\mathbf{V}_{mn}(\mathbf{k}_\perp; t) = \sum_{p,q} C_{qm}^*(\mathbf{k}_\perp; t) \mathbf{v}_{qp}(\mathbf{0}) C_{pn}(\mathbf{k}_\perp; t) + \frac{\hbar}{m} (\mathbf{k}_\perp + \varepsilon t \hat{\mathbf{z}}) \delta_{mn}. \quad (74)$$

Putting $k_\parallel = \varepsilon t$ and defining $D_{mn}(\mathbf{k}_\perp; k_\parallel) \equiv C_{mn}(\mathbf{k}_\perp; t)$ and $\mathbf{W}_{mn}(\mathbf{k}_\perp; k_\parallel) \equiv \mathbf{V}_{mn}(\mathbf{k}_\perp; t)$, we can rewrite Eq. (72) as

$$\frac{dD_{mn}(\mathbf{k}_\perp; k_\parallel)}{dk_\parallel} = -\sum_{q \neq n} D_{mq}(\mathbf{k}_\perp; k_\parallel) \frac{W_{qn}^z(\mathbf{k}_\perp; k_\parallel)}{\omega_{qn}(\mathbf{k}_\perp + k_\parallel \hat{\mathbf{z}})} \quad (75)$$

and Eq. (74) as

$$\mathbf{W}_{mn}(\mathbf{k}_\perp; k_\parallel) = \sum_{p,q} D_{qm}^*(\mathbf{k}_\perp; k_\parallel) \mathbf{v}_{qp}(\mathbf{0}) D_{pn}(\mathbf{k}_\perp; k_\parallel) + \frac{\hbar}{m} (\mathbf{k}_\perp + k_\parallel \hat{\mathbf{z}}) \delta_{mn}. \quad (76)$$

Thus the matrix elements, being independent of the dc field,

can be found once and then reused to calculate spectra as a function of the electric field.

The H_8 , H_{8S} , H_{14NS} , and H_{14} models have remote band parameters, and the presence of the extra k dependence in the Hamiltonian from $H^R(\mathbf{k})$ results in inconsistency if it is not included in the matrix elements. In a crystal, the diagonal elements of the velocity matrix should be proportional to the slopes of the bands, i.e., $\mathbf{v}_{nm}(\mathbf{k}) = \nabla_{\mathbf{k}} \omega_n(\mathbf{k})$. In fact, this extends to the off-diagonal matrix elements so that $\mathbf{v}_{nm}(\mathbf{k}) = \hbar^{-1} \nabla_{\mathbf{k}} \langle n\mathbf{k} | H | m\mathbf{k} \rangle$. When a finite band model includes remote band effects, these identities are no longer satisfied so we restore them by using $\mathbf{v}_{nm}(\mathbf{k}) = \hbar^{-1} \nabla_{\mathbf{k}} H_{\mathbf{k}}$.^{31,35} Thus, when the model contains remote band effects, we use

$$\mathbf{W}_{mn}(\mathbf{k}_\perp; k_\parallel) = \frac{1}{\hbar} \sum_{p,q} D_{qm}^*(\mathbf{k}_\perp; k_\parallel) (\nabla_{\mathbf{k}} H_{\mathbf{k}})_{qp} D_{pn}(\mathbf{k}_\perp; k_\parallel), \quad (77)$$

where $\nabla_{\mathbf{k}} H_{\mathbf{k}}$ is evaluated at $\mathbf{k} = \mathbf{k}_\perp + k_\parallel \hat{\mathbf{z}}$. For the H_{14NR} model, this reduces to Eq. (76), but in the other models, $(\nabla_{\mathbf{k}} H_{\mathbf{k}})_{mn} = \hbar \mathbf{v}_{mn} + (\hbar^2/m) \mathbf{k} \delta_{mn} + (\nabla_{\mathbf{k}} H^R)_{mn}$. While the contribution of the remote band effects to the matrix elements is small for the spectral region considered here, we have included it in the calculations for consistency.

In summary, we use Eq. (76) for H_{14NR} , and Eq. (77) for the H_8 , H_{8S} , H_{14NS} , and H_{14} models, in Eq. (75) to find the velocity matrix elements. The equations are solved numerically using an adaptive Runge-Kutta-Fehlberg solver. The magnitude of the matrix elements at each \mathbf{k} calculated from the differential equation was found to agree within numerical error with the magnitude found by diagonalizing $H_{\mathbf{k}}$. Matrix elements for x -polarized light are shown in Fig. 2 for a particular line through the BZ defined by $\mathbf{k} = (0.0047 \text{ \AA}^{-1}) \hat{\mathbf{x}} + (0.005 \text{ \AA}^{-1}) \hat{\mathbf{y}} + k_\parallel \hat{\mathbf{z}}$. This particular value of \mathbf{k}_\perp was chosen as an example because \mathbf{k} passes near the Γ point at $k_\parallel = 0$, where the upper valence bands become degenerate, and it also passes near a line of spin degeneracy at $k_\parallel = \pm 0.005 \text{ \AA}^{-1}$.

The bands mix where they are nearly degenerate, and this leads to changes in the matrix element amplitudes and phases through the $\mathbf{k} \cdot \mathbf{p}$ interaction. As shown in Fig. 2(a), near degeneracy occurs for the light and heavy hole valence bands near Γ (the region near $k_\parallel = 0$). The mixing leads to strongly varying matrix elements for the heavy and light hole to conduction band transitions, shown in Figs. 2(c) and 2(e) as calculated from H_8 . That the matrix element variation occurs due to near degeneracy can be seen by comparing those plots to Fig. 2(g), which shows the matrix elements calculated from H_8 for the split-off valence to conduction band transition. In contrast with the transitions involving the degenerate valence bands, the split-off valence band to conduction band matrix elements are well behaved and nearly constant near $k_\parallel = 0$. The coupling between nearly degenerate light hole and heavy hole bands, shown in Fig. 2(i), enters the calculation of the FKE through the matrix S and the evolution matrix L . The dc field causes transitions between the nearly degenerate bands due to the nonzero matrix element between them.

In the 14-band models, the bands are spin split by the coupling P'_0 of the lower conduction bands to the upper con-

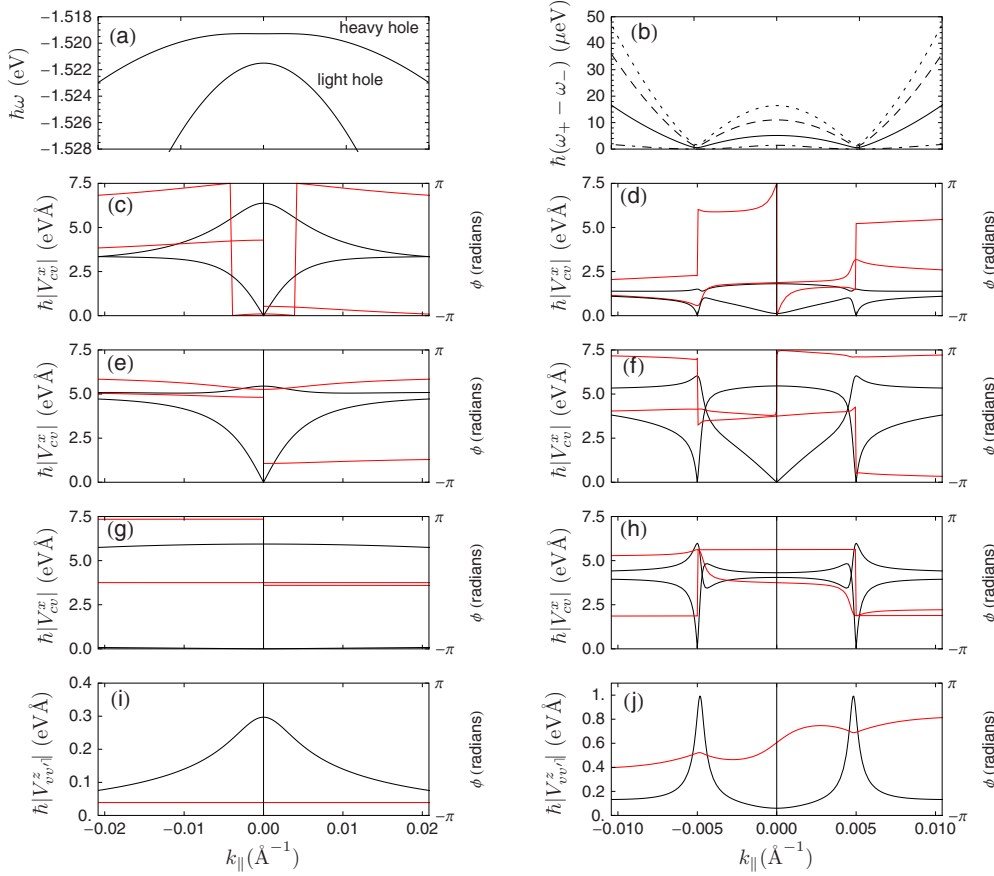


FIG. 2. (Color online) Matrix elements for $\mathbf{k}=(0.0047 \text{ \AA}^{-1})\hat{\mathbf{x}}+(0.005 \text{ \AA}^{-1})\hat{\mathbf{y}}+k_{||}\hat{\mathbf{z}}$. The left (right) side shows the matrix elements for H_8 (H_{14NS}). (a) Valence band dispersion for H_8 near the Γ point. (b) Difference in energy between spin split bands in the H_{14NS} model. Plotted are the splittings for conduction bands (solid), split-off valence bands (dashed), light hole bands (dotted), and heavy hole bands (dash-dot). [(c)–(h)] Magnitude (black, left axis) and phase (red or gray, right axis) of $V_{cv}^x=|V_{cv}^x|e^{i\phi}$. The matrix elements for two out of the four possible pairs of bands are plotted. (c) Heavy hole valence to conduction band from H_8 . (d) Heavy hole to conduction band from H_{14NS} . (e) Light hole to conduction band from H_8 . (f) Light hole to conduction band from H_{14NS} . (g) Split off to conduction band from H_8 . (h) Split off to conduction band from H_{14NS} . [(i) and (j)] Matrix element $|V_{vv}^z|e^{i\phi}$ between light and heavy-hole bands. The matrix element for one out of the four possible band pairs is plotted. (i) Light-hole to heavy-hole band from H_8 . (j) Light-hole to heavy-hole band from H_{14NS} .

duction bands and by C_k and Δ^- . Spin degeneracy occurs along high symmetry directions in the BZ. The spin splittings are plotted in Fig. 2(b) for the valence bands and lower conduction bands, calculated using the H_{14NS} model. When \mathbf{k} nears lines of degeneracy, strong mixing between spin split bands occurs. This can be seen in Figs. 2(d), 2(f), and 2(h), near $k_{||}=\pm 0.005 \text{ \AA}^{-1}$, where \mathbf{k} passes near the $\langle 111 \rangle$ direction. Along $\langle 111 \rangle$ and $\langle 100 \rangle$, spin-split bands become degenerate in the H_{14NS} model (the degeneracy along $\langle 111 \rangle$ is lifted for some pairs of bands in H_{14} because $\Delta^- \neq 0$ but the degeneracy along $\langle 001 \rangle$ remains³³). For the heavy and light hole bands, as in the eight-band models, there are additional effects due to the degeneracy at the Γ point. The mixing at $k_{||}=\pm 0.005 \text{ \AA}^{-1}$ is also evidenced in the strong matrix element between the light hole and heavy hole bands at those wavevectors, as shown in Fig. 2(j). This coupling appears for all pairs of bands in the 14-band models and must be accounted for in the calculation of the FKE.

C. Calculation of band coupling

To find the matrix m , we solve Eq. (46) with initial condition Eq. (47), using the matrix elements calculated from

Eq. (77) in S and the band energies in T . The matrix m oscillates at the frequency differences between bands ω_{mn} . For numerical convenience, we go into an interaction picture, at each \mathbf{k}_{\perp} defining

$$\tilde{m}(\mathbf{k}_{\perp}; t) = e^{i\mathbf{l}(t)/\hbar} m(\mathbf{k}_{\perp}; t), \quad (78)$$

where

$$I_{mn}(t) = \delta_{mn} \hbar \int_0^t \omega_m(\mathbf{k}_{\perp} + \varepsilon t' \hat{\mathbf{z}}) dt'. \quad (79)$$

Recalling $T_{mn}(\mathbf{k}_{\perp}; t) = \delta_{mn} \hbar \omega_m(\mathbf{k}_{\perp} + \varepsilon t \hat{\mathbf{z}})$ and using Eq. (46), we find

$$i\hbar \frac{d\tilde{m}(\mathbf{k}_{\perp}; t)}{dt} = [e^{i\mathbf{l}(t)/\hbar} \mathbf{S}(\mathbf{k}_{\perp}; t) e^{-i\mathbf{l}(t)/\hbar}] \tilde{m}(\mathbf{k}_{\perp}; t). \quad (80)$$

We solve this equation instead of Eq. (46). One can easily show using Eq. (47) that the initial condition remains

$$\tilde{m}_{pn}(\mathbf{k}_{\perp}; 0) = \delta_{pn}.$$

We then use $m(\mathbf{k}_{\perp}; t) = e^{-i\mathbf{l}(t)/\hbar} \tilde{m}(\mathbf{k}_{\perp}; t)$.

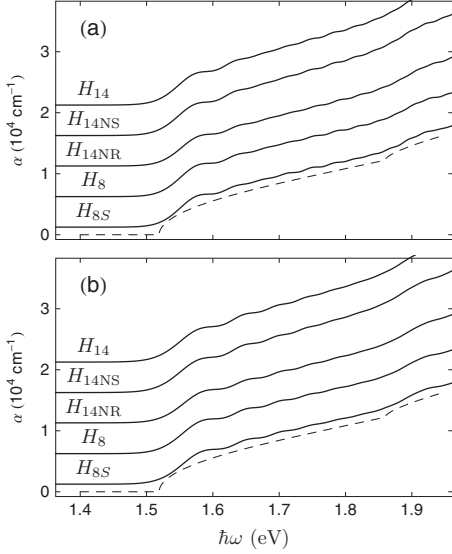


FIG. 3. Calculated absorption spectra for a 66 kV/cm dc field (solid lines) pointing along [001], using the five models for GaAs. The spectra are offset vertically for clarity. (a) Light polarized along [100]. (b) Light polarized along [001]. The dashed line shows the zero-field absorption spectrum for H_{8S} .

D. Absorption spectrum results

The integral over \mathbf{k} in Eq. (60), the expression for the absorption without a dc field, is nominally over the entire BZ. In practice, summing over $|\mathbf{k}| < 0.1 \text{ \AA}^{-1}$ is sufficient to calculate the absorption in GaAs for photon energies between the fundamental band gap 1.519 eV and the split-off gap 1.86 eV. We similarly limit the region of integration for the calculation with an electric field. We solve the equations for the matrix elements over $|k_{\parallel}| < 0.5 \text{ \AA}^{-1}$, then use those to calculate $m(\mathbf{k}_{\perp}; t)$ for $|t| < 0.5 \text{ \AA}^{-1}/\varepsilon$, and finally perform the integration in Eq. (59) over $|\mathbf{k}_{\perp}| < 0.1 \text{ \AA}^{-1}$. We sum over the six valence bands and two lowest energy conduction bands, as we are interested here only in the absorption near the fundamental band edge. This is a computationally intensive calculation. As an example, on an AMD Athlon™ 64 3800+ processor, calculation of the integrand in Eq. (59), for one value of \mathbf{k}_{\perp} and for $E_{\text{dc}} = 66.7 \text{ kV/cm}$, takes 3.3 s for the eight-band models and 19.4 s for the 14-band models. The calculation takes longer the smaller the electric field because of the finer step size required to solve Eq. (80). We sum over $\sim 2 \times 10^5$ values of \mathbf{k}_{\perp} , splitting the work among many computers.

Calculated absorption spectra are shown in Fig. 3. The dc electric field, with strength 66 kV/cm, is assumed to be along the [001] crystal direction. Absorption spectra using the four models with the optical field \mathbf{E}_{opt} pointing along [001] are shown in Fig. 3(a). Figure 3(b) shows the absorption spectrum for an optical field along [100]. For $\mathbf{E}_{\text{opt}} \perp \mathbf{E}_{\text{dc}}$, the Franz-Keldysh oscillations show beats due to the different reduced masses of heavy and light holes, seen in electroreflectance and photorefectance experiments on GaAs (Refs. 36 and 37) and other semiconductors¹⁰ for critical points of the same symmetry. For $\mathbf{E}_{\text{opt}} \parallel \mathbf{E}_{\text{dc}}$, only the light hole bands contribute to the oscillations. Our results on the polarization

dependence are qualitatively consistent with a previous calculation⁸ and electroabsorption data on GaAs.³⁸

There is very little visible difference among the spectra calculated using H_{8S} , H_8 , H_{14NS} , and H_{14} . The H_{14NR} model, with different effective masses, shows a slightly different Franz-Keldysh oscillation period but the spectral shape is not qualitatively different from the other models. The shape of the zero-field spectrum is somewhat different for the H_{14NS} and H_{14} models because of the different band dispersion for large k . We have performed calculations of the FKE spectrum for fields from 16.5 kV/cm to 66 kV/cm using the eight-band models, and from 33 kV/cm to 66 kV/cm for the 14-band models. In Sec. IV, we discuss the results in detail.

E. Effects of the interband coupling

The proper way to treat degenerate bands in the presence of an electric field has been the subject of many studies, both within the Franz-Keldysh effect literature^{10,13,39} and beyond.^{40–43} The main question has been how the electric field lifts the valence band degeneracy at the Γ point in crystals with zincblende or diamond structure. In the formalism used here, the electric field couples carriers in nearby bands together as they are accelerated with the coupling arising from the dipole moment between bands in the zero-field Hamiltonian. In spirit, our approach is similar to semiclassical treatments of transport which consider coherent wavepackets and how they interact with electromagnetic fields^{44,45} with the dipole moment $\boldsymbol{\mu}(\mathbf{k}; t)$ between nearly degenerate bands playing the role of a non-Abelian Berry connection. However, while we treat the electromagnetic field classically, we stress that here we treat the electron dynamics fully quantum mechanically.

The absorption spectrum is the result of a sum of the contributions from each possible trajectory an electron's or hole's wavevector can take through the BZ, indexed by \mathbf{k}_{\perp} [recall Eq. (59)]. Within each trajectory, the amplitude and relative phase of the matrix elements, along with the effects from coupling to nearby bands, have an effect on the absorption spectrum. Keldysh, Konstantinov, and Perel' (henceforth referred to as KKP) argued that the light hole contribution to the FKE for photon energy below the band gap in GaAs can be calculated to a good approximation assuming that the heavy and light hole bands are decoupled.¹¹ That is, the spectrum is consistent with a calculation using the value of the matrix elements near Γ for $\mathbf{k} \parallel \mathbf{E}_{\text{dc}}$ and neglecting the interband coupling. Aspnes later argued that the same approximation works for both light and heavy holes for energies far above the band gap.¹⁰ For $\mathbf{E}_{\text{opt}} \parallel \mathbf{E}_{\text{dc}}$, the KKP approximation correctly predicts that only light holes contribute, while for $\mathbf{E}_{\text{opt}} \perp \mathbf{E}_{\text{dc}}$, it predicts a 1:3 ratio for the relative contribution from light and heavy holes, respectively.

To illustrate the effects of interband coupling, we here examine the “one-trajectory” absorption for light polarized along [100] and the dc field along [001], which is proportional to

$$\sum_{cv} |\theta_{cv\mathbf{k}_{\perp}}^x(\omega)|^2.$$

This is shown in Fig. 4 using the H_8 and H_{14NS} models, for the same value $\mathbf{k}_{\perp} = (0.0047 \text{ \AA}^{-1})\hat{x} + (0.005 \text{ \AA}^{-1})\hat{y}$ as was

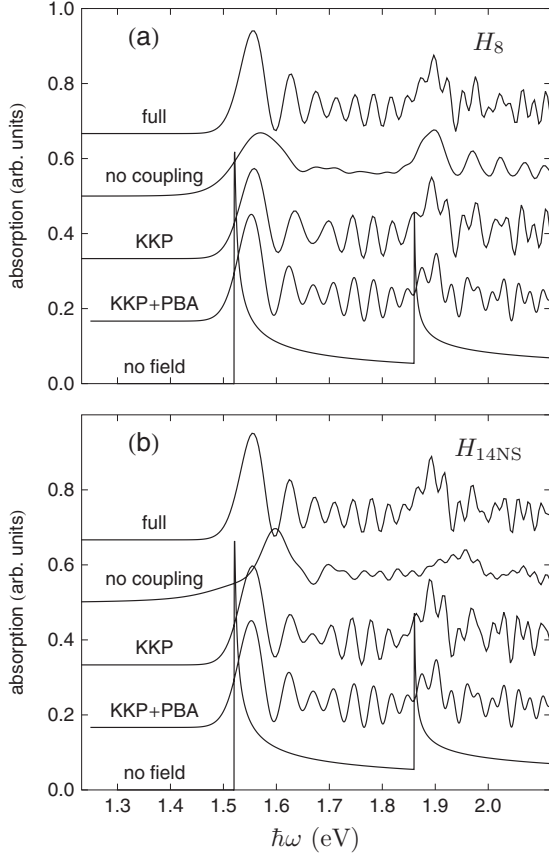


FIG. 4. One-trajectory absorption spectrum for $\mathbf{k}_\perp = (0.0047 \text{ \AA}^{-1})\hat{x} + (0.005 \text{ \AA}^{-1})\hat{y}$, with light polarized along [100], assuming a 66 kV/cm dc field in the [001] direction. (a) H_8 model. (b) H_{14NS} model. Plotted, from bottom to top, are the calculated spectrum without a dc field; with a dc field in the PBA using known effective masses and KKP matrix elements (Refs. 10 and 11); with full band dispersion and KKP matrix elements; with band dispersion and matrix elements but neglecting interband coupling; and the full calculation. Spectra have been offset vertically for clarity.

used for Fig. 2. The bottom trace labeled “no field” shows, for reference, the absorption along that trajectory with no electric field. That is calculated in Appendix D; the spectrum shown is $|\gamma_{cv\mathbf{k}}^j|^2 \delta[\omega - \omega_{cv}(\mathbf{k})]$ integrated over k_\parallel , where $\gamma_{cv\mathbf{k}}^j$ is given by Eq. (61). The next trace from the bottom, labeled “KKP+PBA,” is the parabolic band approximation expression (derived in Appendix E), proportional to

$$\sum_{cv} |V_{cv}^x|^2 \text{Ai}^2\left(-\frac{\omega - \omega_g}{\Omega_{cv}}\right),$$

where $\Omega_{cv} = (\hbar\epsilon^2/2\mu_{cv})^{1/3}$ is the electro-optic frequency with μ_{cv} the reduced mass between valence band v and conduction band c . We assume the KKP spectral weighting of 1/4 light holes, 3/4 heavy holes for the matrix elements. The trace third from the bottom, labeled “KKP,” is the absorption calculated using the band dispersion from the $\mathbf{k}\cdot\mathbf{p}$ model and the KKP matrix elements. The trace second from the top, labeled “no coupling,” is the absorption calculated using the matrix elements shown in Fig. 2 but neglecting interband

coupling between bands, found by setting $S(\mathbf{k};t)=0$ in Eq. (46). The top trace, labeled “full” is the one-trajectory absorption spectrum from the full calculation. We find that the full calculation, including coupling between bands, is indeed remarkably similar to the KKP result.

Comparing the “KKP” curves to the “KKP+PBA” curves in Fig. 4 shows the effects of nonparabolicity to be relatively minor, primarily affecting the lineshape of the beat in the spectrum near 1.68 eV. Comparing those to the full calculation, the primary effects are (a) the position of the beat between light and heavy holes shifts upward in energy, and (b) the amplitude of the oscillations is somewhat smaller in the full calculation than in the KKP approximation. The strong distortion of the spectrum seen when the coupling between bands is neglected arises mainly from the strong variation of the matrix elements. In the case of the H_8 model, shown in Fig. 4(a), the split-off valence bands do not interact with other bands, and as a result, the spectrum near $E_g + \Delta_0 = 1.86$ eV is not noticeably affected by the neglect of interband coupling. In the case of the H_{14NS} model, shown in Fig. 4(b), there is additional coupling between spin up and spin down bands. There the interband coupling must be included even for the split-off valence and conduction bands. While the valence band coupling has been noted previously, we believe the importance of the spin coupling in the FKE has not previously been discussed. In each case, the effect of the interband coupling leads to spectra that are qualitatively consistent with uncoupled bands, using constant matrix elements.

IV. RESULTS

In this section, we examine in detail the Franz-Keldysh absorption spectra calculated from the models. Previous theoretical efforts have been focused on the FKE spectrum below the band gap^{8,11} and the effect of band nonparabolicity on the Franz-Keldysh oscillation period.^{8,9} Here we use our models to calculate the dependence of the FKE spectrum on the direction of the dc field. We concentrate on two effects, one related to the warping of the valence bands and the other to the k -dependent spin splitting of the bands in the 14-band models due to broken inversion symmetry. To show clearly the effect of the electric field on the absorption, we concentrate in the following on the electroabsorption spectrum, the difference $\Delta\alpha(\omega)$ between the absorption with and without a dc field. Differential quantities such as $\Delta\alpha(\omega)$ are what is typically measured in electromodulation experiments. In Fig. 5, we compare the electroabsorption in the PBA and using the $\mathbf{k}\cdot\mathbf{p}$ models.

The period of the Franz-Keldysh oscillations is related to the field strength and the reduced effective mass. For the case of parabolic bands and no broadening,³ $\Delta\alpha(\omega) \propto F[(E_g - \hbar\omega)/\hbar\Omega]$, where the electro-optic function

$$F(x) = \frac{1}{\pi} \{ [\text{Ai}'(x)]^2 - x \text{Ai}^2(x) \} - (-x)^{1/2} H(-x), \quad (81)$$

where $\text{Ai}(x)$ is the Airy function and $H(x)$ is the Heaviside function. Because the theory does not include scattering and thus has no source of dephasing, sharp features appear at E_g

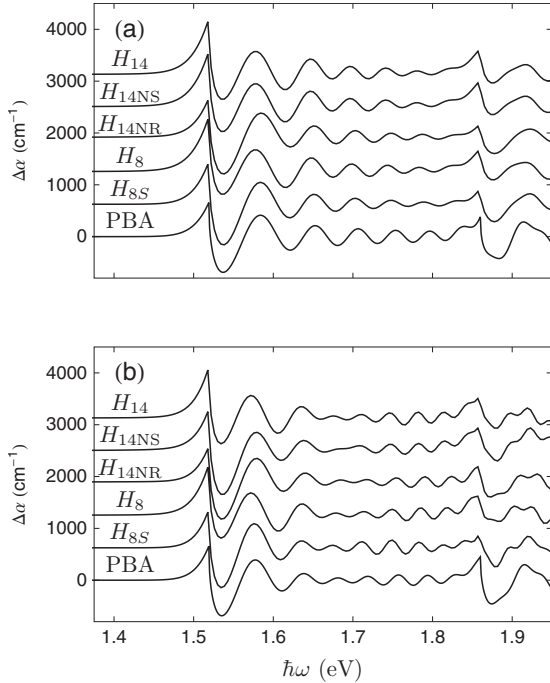


FIG. 5. Differential absorption calculated using the various models for an electric field of strength 66 kV/cm oriented along [001]. (a) Optical field pointing along [100]. (b) Optical field pointing along [001]. Spectra have been offset vertically for clarity.

and $E_g + \Delta_0$. Dephasing would tend to smooth these features and also damp out the Franz-Keldysh oscillations at higher energies. The effects of dephasing on the FKE is an important topic which has been noted¹⁷ but has only been included in most theoretical treatments as a phenomenological broadening parameter.⁴ The Coulomb interaction, also neglected here, changes the shape of the band-edge features as well.^{15,16,46}

For $\hbar\omega \gg E_g$, the asymptotic limit of $F(x)$ for $x \ll 0$ yields

$$\Delta\alpha(\omega) \approx \frac{K}{\hbar\omega - E_g} \cos \left[\frac{4}{3} \left(\frac{\hbar\omega - E_g}{\hbar\Omega_{cv}} \right)^{3/2} + \phi \right], \quad (82)$$

where K and ϕ are constants. Thus, to the extent that the Airy function theory applies, the energies of the oscillation extrema when plotted as a function of $s = (\hbar\omega - E_g)^{3/2}$ should fit to a line, the slope of which is related to the effective mass. This sort of analysis has been used previously for numerical calculations⁸ and experiments.^{47,48} When there are two Franz-Keldysh oscillation periods present, as in GaAs for $\mathbf{E}_{dc} \perp \mathbf{E}_{opt}$, a plot of the extrema versus s yields information about the stronger of the two signals (from the heavy holes), but not the weaker. To extract more information, one could do nonlinear fits of the spectrum to two Airy functions, one for each type of hole.¹⁰ We instead use a simpler, more versatile approach based on the fact that the Fourier transform of the stretched electroabsorption spectrum $\Delta\alpha(s)$ has peaks at $4/[3(\hbar\Omega_{cv})^{3/2}]$.⁴⁹ Thus, the Fourier transform shows separate peaks corresponding to the heavy and light hole oscillations, allowing examination of both electro-optic frequencies and the relative strengths of the peaks. It is also less

sensitive to the precise lineshape than fitting. We only use the magnitude of the Fourier spectrum here; information about the phase of the oscillations can also be extracted using the complex Fourier spectrum.^{50,51}

In GaAs the electroreflectance spectrum is caused mainly by changes in the real part of the dielectric constant. We do not calculate that here but it could be found from the imaginary part through the Kramers-Kronig relations.⁴ It must also be kept in mind that in many experiments, particularly those using photorefectance, the modulation is not between zero electric field (flat band) to nonzero electric field but rather between two finite field values.^{7,50} Still, the same basic trends found here for the Franz-Keldysh oscillation period and the relative light hole-heavy hole spectral weight in the absorption spectrum should hold for the reflectance spectrum as well.

A. Band warping

It has been found previously that the Franz-Keldysh oscillation period calculated using an eight-band $\mathbf{k} \cdot \mathbf{p}$ model is consistent with the Airy function theory, using the effective mass in the direction of the dc field to calculate the electro-optic frequency.⁸ The spectrum depends on the motion of the particle throughout its trajectory so the overall shape of the band matters more than the local curvature.^{8,9} The primary effect of nonparabolicity is on the damping rate of the oscillations as the photon energy is increased. For this reason the Franz-Keldysh effect is well suited for measuring the dependence of the effective mass on direction, often called “band warping.” Intuitively, the Franz-Keldysh oscillations for the field oriented along a particular direction should give the effective mass along that direction and this has in fact been used to interpret experimental data¹⁰ but there has been no theoretical study of the effect.

In GaAs and other materials with zincblende or diamond symmetry, warping is particularly strong for holes. In Fig. 6, we show the calculated electroabsorption spectra and Fourier transform using H_8 for \mathbf{E}_{dc} (field strength 16.5 kV/cm) oriented along various directions. The oscillation period depends on the DC field direction for both bands, with the difference for the light hole band, which dominates the spectrum for $\mathbf{E}_{dc} \parallel \mathbf{E}_{opt}$ [shown in Figs. 6(a) and 6(b)], harder to observe than the more strongly warped heavy hole bands, which appear for $\mathbf{E}_{dc} \perp \mathbf{E}_{opt}$ [shown in Figs. 6(c) and 6(d)]. The position of the heavy hole-light hole beat in the spectrum for $\mathbf{E}_{dc} \perp \mathbf{E}_{opt}$, shown in Fig. 6(c), depends on the direction of the dc field due to the warping. A change in the position of this beat is probably more easily observable in experiments than changes in the Franz-Keldysh oscillation amplitude. The dependence on field direction is more obvious in the Fourier transform of the above-gap spectra, shown in Figs. 6(b) and 6(d).

To study the dependence of the spectrum on the field direction more quantitatively, we extract the effective mass from the position of the peak in the Fourier transform shown in Figs. 6(b) and 6(d). We use a Gaussian window to remove artifacts from the Fourier transform due to the cutoff at $\hbar\omega = E_g + \Delta_0$, and we zero out the region of the electroabsorp-

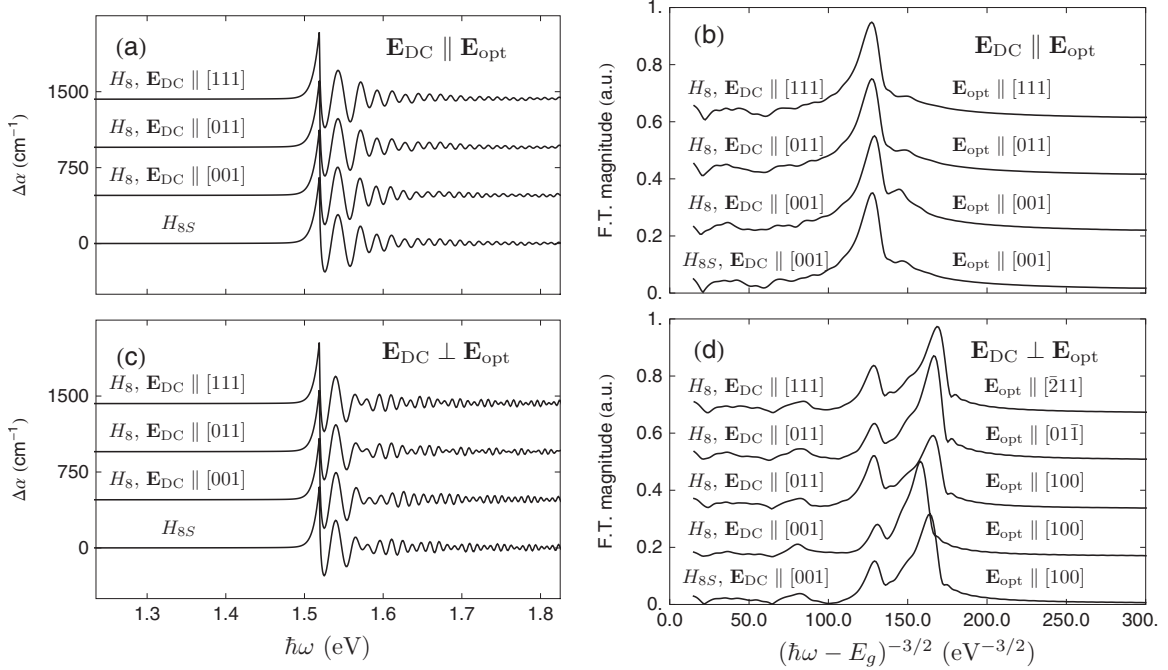


FIG. 6. Effect of warping on the Franz-Keldysh spectrum. The differential absorption and the Fourier transform of $\Delta\alpha$ as a function of $s=(\hbar\omega-E_g)^{3/2}$ (for $s>0$), as described in the text, are plotted for a 16.5 kV/cm field oriented along [001], [110], and [111]. (a) Differential absorption for the optical field parallel to dc field. (b) Fourier transform of the data in (a). (c) Differential absorption for the optical field perpendicular to dc field. For $\mathbf{E}_{dc}\parallel[011]$, the spectrum is shown for $\mathbf{E}_{opt}\parallel[100]$. (d) Fourier transform of the data in (c). Spectra have been offset vertically for clarity.

tion spectrum near the band gap, where the asymptotic limit that led to Eq. (82) is not valid. Because nonparabolicity results in a gradual change in the oscillation period as $\hbar\omega-E_g$ increases,^{8,9} the peaks display some asymmetry. We have not attempted to account for this in our analysis, as we are more interested in the rough trends. The results are summarized in Table II. The effective masses for the light holes (lh) and heavy holes (hh) calculated using the Luttinger parameters in the H_{8S} model are, along any direction, $m_{lh}=0.073m_e$ and $m_{hh}=0.534m_e$. Those calculated using the H_8 model are, along $\langle 001\rangle$, $m_{lh}=0.079m_e$, $m_{hh}=0.347m_e$; along $\langle 011\rangle$, $m_{lh}=0.071m_e$, $m_{hh}=0.634m_e$; and along $\langle 111\rangle$, $m_{lh}=0.069m_e$, $m_{hh}=0.834m_e$.²⁰ Similar trends can be seen in the effective masses extracted from the peaks in the Fourier transform of the calculated spectra. Disagreement in the numbers between the masses expected from the model and those extracted from the FKE spectra is probably caused by the chirping of the oscillation period due to nonparabolicity, though effects of the interband coupling near the Γ point could also contribute.

We also analyzed the relative strength of the heavy and light hole oscillations. We integrated the peaks in the Fourier transform, normalizing by the strength of the light hole peak for $\mathbf{E}_{dc}\parallel\mathbf{E}_{opt}\parallel\langle 001\rangle$ to yield the spectral weight. For $\mathbf{E}_{dc}\perp\mathbf{E}_{opt}$, the KKP approximation predicts a 3:1 ratio for the spectral weight of the heavy holes to that of the light holes. Using the spherical H_{8S} model, we extract a ratio of 3.44 from the calculated spectrum. The ratio depends on the direction of the dc field using H_8 , presumably due to band warping effects. For the dc field along [001] and the optical field along [100], we find a ratio of 4.2, close to the value of

4.1 reported in a photoreflectance experiment on GaAs.⁵¹

Obviously, caution should be used in comparing the calculations here to experiments because we have neglected the Coulomb interaction and scattering. The latter effect tends to damp out the oscillations, and coupled with the chirp in the Franz-Keldysh oscillations due to nonparabolicity, could change the peak in the Fourier transform, affecting the extracted effective mass. Still, given that experiments at low

TABLE II. Effective masses extracted from the electro-optic frequencies Ω_{cv} derived from the peak of the Fourier transform and spectral weights (relative to the weight of the light hole peak for $\mathbf{E}_{dc}\parallel\mathbf{E}_{opt}\parallel[001]$) of the heavy and light hole oscillations as a function of the direction of the dc field (of magnitude 16.5 kV/cm) and the optical field.

Model	Direction		m_{lh}/m_e	m_{hh}/m_e	Spectral weight	
	\mathbf{E}_{dc}	\mathbf{E}_{opt}			lh	hh
H_{8S}	[001]	[001]	0.071		1.02	
		[100]	0.076	0.459	0.38	1.31
H_8	[001]	[001]	0.076		1.0	
		[100]	0.078	0.28	0.30	1.25
	[011]	[011]	0.071		1.04	
		[100]	0.073	0.57	0.51	1.16
	[111]	[0 $\bar{1}$ 1]	0.073	0.57	0.35	1.54
		[1 $\bar{1}$ 1]	0.071		1.05	
		[$\bar{1}$ 01]	0.073	0.75	0.48	1.35
		[1 $\bar{2}$ 1]				

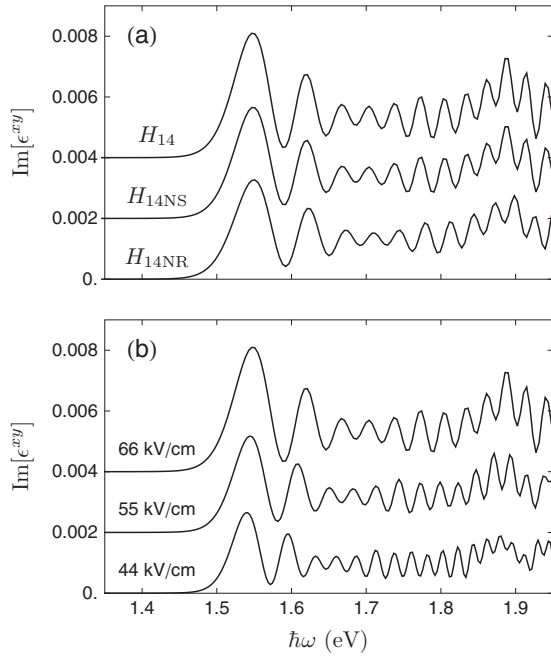


FIG. 7. Linear FKE calculated using H_{14} . $\text{Im}[\epsilon^{xy}]$ is plotted for a dc field along \hat{z} . Spectra have been offset vertically for clarity. (a) Spectra at a field strength of 66 kV/cm for H_{14NR} , H_{14NS} , and H_{14} . (b) Spectra as a function of field strength, as calculated from H_{14NS} .

temperature show many oscillations,^{46,48} we believe the directional dependence of the oscillation period and the light hole-heavy hole relative spectral weight should be observable. Experiments that show many Franz-Keldysh oscillations involve the use of specially grown heterostructures with built-in fields along (001).⁷ Samples with that orientation are what is typically grown by molecular beam epitaxy so another technique may need to be found in order to study these orientation effects. We note that a new technique for transverse electroreflectance,⁵² which overcomes the field nonuniformity commonly found in experiments using that geometry and does not rely on doped samples, may be a more versatile technique for these sorts of experiments.

B. Odd FKE

In the 14-band model for GaAs, the coupling between the s -like lower and p -like upper conduction bands results in k -linear terms in the Hamiltonian.³³ These produce a \mathbf{k} -dependent spin splitting (present only in the absence of inversion symmetry), which results in a change in the absorption spectrum that depends on the sign of the dc field.^{53,54} From the standpoint of nonlinear optics, the lowest order term, linear in E_{dc} , arises from $\chi^{(2)}$, and consequently this is sometimes referred to as the Pockels effect. But our concern here is the change in the absorption coefficient, not in the refractive index. For zincblende symmetry the only nonzero tensor element is xyz and so, for example, an electric field along the \hat{z} direction produces a difference in absorption for \hat{x} and \hat{y} polarized light.⁴⁷ This is indeed what we find, shown in Fig. 7. Like the even Franz-Keldysh spectra for $\mathbf{E}_{opt} \perp \mathbf{E}_{dc}$, the odd FKE spectrum displays heavy hole-

light hole beats. We found that the three 14-band models did not produce wildly different odd FKE spectra, as shown in Fig. 7(a). This suggests that the odd FKE arises primarily from the previously mentioned coupling P'_0 between the lower and upper conduction bands rather than from coupling to faraway bands, taken into account here through the remote parameter C_k .

The shape of the odd FKE spectrum is oscillatory, but the spectrum oscillates about a nonzero value (proportional to E_{dc}) that should be measurable at room temperature in the presence of broadening. The odd FKE has been observed in GaAs in reflectance measurements for photon energies around the E_1 gap near 3 eV.^{55,56} In experimental techniques such as photoreflectance that use built-in electric fields, the electric field is modulated about a large, finite value, making it difficult to isolate the odd from the even effects. This is also a problem in transverse experiments because of space charge effects. The most thorough study of the effect near the fundamental edge we have found was done by Belogurov and Shaldin,⁵⁷ who tried to carefully separate effects due to field nonuniformity, which depended on the position of the light on the sample, from the odd FKE. They do not provide a quantitative measurement of the differential absorption, however. Finally, we note that experiments are complicated by surface and other effects that also break inversion symmetry and cause changes in the reflectance which are odd in the electric field.^{58–61}

V. CONCLUSION

In summary, we have developed an independent-particle theory of the Franz-Keldysh effect using basis states that take into account both intraband motion due to the dc field and interband coupling between nearly degenerate states. The theoretical framework is designed in such a way that the differential absorption spectrum may easily be calculated. The interband coupling between bands is an extremely important part of the Franz-Keldysh effect in GaAs, both for the valence bands near the Γ point and between spin split bands. Without proper inclusion of the coupling, the variation of the phase of the matrix elements within the Brillouin zone causes distortion and washing out of the Franz-Keldysh oscillations. While the coupling near the valence band degeneracy has been previously discussed, its implications are not widely recognized, and we believe the additional coupling between spin degenerate bands has not been previously discussed.

We calculated the electroabsorption spectrum using a 14-band $\mathbf{k} \cdot \mathbf{p}$ model and four submodels derived from it by neglecting various parameters. Our calculations predict a dependence of the spectrum on the orientation of the dc field with respect to the crystal axes due to valence band warping. For the dc field along the [001] direction and the optical field along [100], a geometry typical of photoreflectance experiments, our theory correctly predicts the ratio of the oscillation amplitudes due to light and heavy holes observed in experiments.⁵¹ We predict that ratio to depend strongly on the direction of the dc field; this has not yet been explored experimentally. The 14-band Hamiltonian has additional

terms arising from bulk inversion asymmetry that lead to the odd (in the dc field) Franz-Keldysh effect, which to our knowledge has not been calculated before in any detail. The linear change in the absorption spectrum with electric field is closely related to the Pockels effect, technologically important in electro-optic modulators and terahertz detectors.

While we presented results from a $\mathbf{k} \cdot \mathbf{p}$ model for the band structure, the framework could be used to calculate using other types of models as well. It can also be generalized to calculate nonlinear optical effects such as multiphoton absorption and interferences between one- and two-photon absorption.⁶² It could also easily be adapted to numerical calculations of the Franz-Keldysh effect in nanostructures.⁶³ The fact that even an independent-particle theory displays so much rich physics suggests that there is much lurking beneath the surface and we hope that interest in the Franz-Keldysh effect will be rekindled as better theories are developed. Finally, we note that the Franz-Keldysh effect is really an ultrafast phenomenon, relying on the acceleration of carriers on a subpicosecond time scale. While ultrafast experiments have taken advantage of the FKE to measure electric field dynamics,^{64,65} there is potentially much more to be done in this area.

ACKNOWLEDGMENTS

We thank S. T. Cundiff for many discussions and all members of the Cundiff research group at JILA for allowing the use of their computational resources. J.E.S. thanks the Natural Sciences and Engineering Research Council of Canada (NSERC) for support.

APPENDIX A: DERIVING THE EFFECTIVE INTERACTION HAMILTONIAN

In this appendix, details of the derivation that leads to Eqs. (32) and (40) are given. We first determine the dynamics of the operators $b_{n\mathbf{k}}(t)$ for $t > t_{\text{initial}}$ [see Eq. (27)]. There will be contributions from the time dependence of $\bar{\chi}_n^*(\mathbf{k}; \mathbf{x})$ and from that of $\psi^H(\mathbf{x}, t)$; the latter is a Heisenberg operator so we can use Eq. (24) and rewrite the results in terms of a commutator of $b_{n\mathbf{k}}(t)$ with $H^H(t)$. In all we find

$$i\hbar \frac{db_{n\mathbf{k}}(t)}{dt} = i\hbar \int \frac{d\bar{\chi}_n^*(\mathbf{k}; \mathbf{x})}{dt} \psi^H(\mathbf{x}, t) d\mathbf{x} + [b_{n\mathbf{k}}(t), H^H(t)]. \quad (\text{A1})$$

For the time derivative of $\bar{\chi}_n^*(\mathbf{k}; \mathbf{x})$ use the complex conjugate of Eq. (18) and the complex conjugate of Eq. (11) for the time derivative of $\bar{\phi}_n^*(\mathbf{k}; \mathbf{x})$, together with $\boldsymbol{\mu}_{mn}^*(\mathbf{k}; t) = \boldsymbol{\mu}_{nm}(\mathbf{k}; t)$ from Eqs. (10) and (12). Using the complex conjugate of Eq. (19) to eliminate the $\bar{\phi}_n^*(\mathbf{k}; \mathbf{x})$ in terms of the $\bar{\chi}_n^*(\mathbf{k}; \mathbf{x})$, and the definition [Eq. (27)] to identify expressions for $b_{n\mathbf{k}}(t)$, the result is

$$i\hbar \frac{db_{n\mathbf{k}}(t)}{dt} = [b_{n\mathbf{k}}(t), H^H(t)] + i\hbar \sum_{p,q} \frac{dL_{pn}^*(\mathbf{k}; t)}{dt} L_{pq}(\mathbf{k}; t) b_{q\mathbf{k}}(t) - \sum_{p,m,q} L_{mn}^*(\mathbf{k}; t) L_{pq}(\mathbf{k}; t) b_{q\mathbf{k}}(t) \boldsymbol{\mu}_{mp}(\mathbf{k}; t) \cdot \mathbf{E}_{\text{dc}}(t).$$

Note now that if we introduce an effective Heisenberg Hamiltonian

$$H_{\text{eff}}^H(t) = H^H(t) + i\hbar \sum_{n,p,q,\mathbf{k}} \frac{dL_{pn}^*(\mathbf{k}; t)}{dt} L_{pq}(\mathbf{k}; t) b_{n\mathbf{k}}^\dagger(t) b_{q\mathbf{k}}(t) - \sum_{n,p,m,q,\mathbf{k}} L_{mn}^*(\mathbf{k}; t) L_{pq}(\mathbf{k}; t) b_{n\mathbf{k}}^\dagger(t) b_{q\mathbf{k}}(t) \times \boldsymbol{\mu}_{mp}(\mathbf{k}; t) \cdot \mathbf{E}_{\text{dc}}(t) \quad (\text{A2})$$

the dynamics [Eq. (A1)] for $b_{n\mathbf{k}}(t)$ are given by the Heisenberg-like equations

$$i\hbar \frac{db_{n\mathbf{k}}(t)}{dt} = [b_{n\mathbf{k}}(t), H_{\text{eff}}^H(t)]. \quad (\text{A3})$$

We can write $H^H(t)$, and thus $H_{\text{eff}}^H(t)$, in terms of the $b_{m\mathbf{k}}(t)$ and $b_{n\mathbf{k}}^\dagger(t)$. To do this, use Eq. (26) in Eq. (25), use Eq. (18) to write the results in terms of the matrix elements of the $\{\bar{\phi}_p(\mathbf{k}; \mathbf{x})\}$, and recall that matrix elements of $\mathcal{H}(t)$ only connect states of the same \mathbf{k} . Using Eqs. (9), (10), and (25) $H^H(t)$ then reduces to

$$H^H(t) = \sum_{n,q,m,p,\mathbf{k}} b_{n\mathbf{k}}^\dagger(t) b_{q\mathbf{k}}(t) L_{mn}^*(\mathbf{k}; t) \hbar \omega_m(\mathbf{k} + \mathbf{K}) \delta_{mp} L_{pq}(\mathbf{k}; t) - \frac{e}{c} \mathbf{A}_{\text{opt}}(t) \cdot \sum_{n,q,m,p,\mathbf{k}} b_{n\mathbf{k}}^\dagger(t) b_{q\mathbf{k}}(t) \times L_{mn}^*(\mathbf{k}; t) \mathbf{V}_{mp}(\mathbf{k}; t) L_{pq}(\mathbf{k}; t). \quad (\text{A4})$$

Choosing the evolution matrix $L(\mathbf{k}; t)$ so that it satisfies Eq. (35), the full $H_{\text{eff}}^H(t)$ then reduces to

$$H_{\text{eff}}^H(t) = -\frac{e}{c} \mathbf{A}_{\text{opt}}(t) \cdot \sum_{n,q,\mathbf{k}} b_{n\mathbf{k}}^\dagger(t) b_{q\mathbf{k}}(t) \tilde{\mathbf{V}}_{nq}(\mathbf{k}; t), \quad (\text{A5})$$

where $\tilde{\mathbf{V}}_{nq}(\mathbf{k}; t)$ is given by Eq. (34).

Thus the dynamics for $b_{n\mathbf{k}}(t)$ are given by Eqs. (A3) and (A5), together with the condition that $b_{n\mathbf{k}}(t) = b_{n\mathbf{k}}$ for $t < t_{\text{initial}}$, where the $b_{n\mathbf{k}}$ satisfy Eqs. (29) and (30) for our ket $|\Psi^H\rangle$. Finally, note that for $t < t_{\text{initial}}$ Eq. (35) reduces to

$$i\hbar \frac{dL_{pn}(\mathbf{k}; t)}{dt} = \hbar \omega_p(\mathbf{k} + \mathbf{K}^o) L_{pn}(\mathbf{k}; t)$$

a solution of which is indeed Eq. (20). So as $\mathbf{E}_{\text{dc}}(t)$ is turned on at $t = t_{\text{initial}}$ the $L_{pn}(\mathbf{k}; t)$ will evolve in a smooth way.

We now go into an interaction picture by introducing an evolution operator $\hat{U}_{\text{eff}}(t)$ that satisfies the initial condition $\hat{U}_{\text{eff}}(t_{\text{initial}}) = 1$ and

$$i\hbar \frac{d\hat{U}_{\text{eff}}(t)}{dt} = \hat{U}_{\text{eff}}(t) H_{\text{eff}}^H(t). \quad (\text{A6})$$

Given that $b_{n\mathbf{k}}(t)$ satisfies Eq. (A3) it is easy to see that

$$b_{nk} = \hat{U}_{\text{eff}}(t)b_{nk}(t)\hat{U}_{\text{eff}}^\dagger(t). \quad (\text{A7})$$

Defining an effective interaction operator $H_{\text{eff}}(t)$ according to

$$H_{\text{eff}}(t) = \hat{U}_{\text{eff}}(t)H_{\text{eff}}^H(t)\hat{U}_{\text{eff}}^\dagger(t) \quad (\text{A8})$$

we see that Eq. (A6) can be written in the more usual form

$$i\hbar \frac{d\hat{U}_{\text{eff}}(t)}{dt} = H_{\text{eff}}(t)\hat{U}_{\text{eff}}(t). \quad (\text{A9})$$

From Eq. (A5), using the definition in Eq. (A8) and recalling Eq. (A7), we arrive at Eq. (32).

In calculating the absorption, we will want to consider the number of electrons that are promoted to the conduction band. Combining Eqs. (26) and (18) we have

$$\psi^H(\mathbf{x}, t) = \sum_{n,p,\mathbf{k}} b_{nk}(t)L_{np}(\mathbf{k}; t)\bar{\phi}_p(\mathbf{k}; \mathbf{x}) = \sum_{p,\mathbf{k}} a_{p\mathbf{k}}(t)\bar{\phi}_p(\mathbf{k}; \mathbf{x}),$$

where

$$a_{p\mathbf{k}}(t) = \sum_n b_{nk}(t)L_{np}(\mathbf{k}; t) \quad (\text{A10})$$

is a destruction operator associated with the (time-dependent) state $\bar{\phi}_p(\mathbf{k}; \mathbf{x})$ that describes motion only within band p . Because the matrix $L(\mathbf{k}; t)$ is unitary it is easy to confirm that the operators $a_{p\mathbf{k}}(t)$ satisfy the standard anticommutation relations, $\{a_{p\mathbf{k}}(t), a_{p'\mathbf{k}'}(t)\} = 0$ and $\{a_{p\mathbf{k}}(t), a_{p'\mathbf{k}'}^\dagger(t)\} = \delta_{pp'}\delta_{\mathbf{k}\mathbf{k}'}$, and since our interest is only in the expectation value of the total number of electrons in the conduction bands, we can find that by taking the expectation value of the sum of the number operators $a_{c\mathbf{k}}^\dagger(t)a_{c\mathbf{k}}(t)$, where we sum only over the conduction bands (denoted by c)

$$\begin{aligned} \mathcal{N}_c(t) &= \sum_{c,\mathbf{k}} \langle \Psi^H | a_{c\mathbf{k}}^\dagger(t)a_{c\mathbf{k}}(t) | \Psi^H \rangle \\ &= \sum_{c,n,m,\mathbf{k}} L_{nc}^*(\mathbf{k}; t)L_{mc}(\mathbf{k}; t) \langle \Psi^H | b_{n\mathbf{k}}^\dagger(t)b_{m\mathbf{k}}(t) | \Psi^H \rangle \\ &= \sum_{c,n,m,\mathbf{k}} L_{nc}^*(\mathbf{k}; t)L_{mc}(\mathbf{k}; t) \langle \Psi(t) | b_{n\mathbf{k}}^\dagger b_{m\mathbf{k}} | \Psi(t) \rangle \end{aligned} \quad (\text{A11})$$

leading to Eq. (40) for $t > t_{\text{end}}$.

APPENDIX B: PROPERTIES OF $\mathbf{V}_{mn}(\mathbf{k}; t)$ AND $L(\mathbf{k}; t)$

The vector $\mathbf{V}_{mn}(\mathbf{k}; t)$ is given by Eq. (10) with time dependence residing in $\mathbf{K}(t)$ and also implicitly in the wave functions $\bar{\phi}_n(\mathbf{k}; \mathbf{x})$. From Eq. (15) we can write

$$\mathbf{V}_{mn}(\mathbf{k}_\perp, k_\parallel; t) = \mathbf{v}_{mn}[\mathbf{k}_\perp + \hat{\mathbf{z}}(k_\parallel + \varepsilon t)]e^{i\varphi_{mn}(\mathbf{k}_\perp, k_\parallel; t)}. \quad (\text{B1})$$

To write the expression for $\varphi_{mn}(\mathbf{k}_\perp, k_\parallel; t)$ from Eq. (13), note that from Eq. (14) we have $\boldsymbol{\kappa}' = \mathbf{k}_\perp + k_\parallel \hat{\mathbf{z}} + \varepsilon t' \hat{\mathbf{z}}$ and so $d\boldsymbol{\kappa}' = \varepsilon \hat{\mathbf{z}} dt'$. Since when $\boldsymbol{\kappa}' = \mathbf{k} = \mathbf{k}_\perp + k_\parallel \hat{\mathbf{z}}$ we have $t' = 0$, and when $\boldsymbol{\kappa}' = \mathbf{k} + \mathbf{K}(t) = \mathbf{k}_\perp + k_\parallel \hat{\mathbf{z}} + \varepsilon t \hat{\mathbf{z}}$ we have $t' = t$, we can write Eq. (13) as

$$\varphi_n(\mathbf{k}_\perp, k_\parallel; t) = -\varepsilon \int_0^t \xi_{nn}^z(\mathbf{k}_\perp + k_\parallel \hat{\mathbf{z}} + \varepsilon t' \hat{\mathbf{z}}) dt' \quad (\text{B2})$$

and so [see Eq. (16)], we have

$$\begin{aligned} \varphi_{mn}(\mathbf{k}_\perp, k_\parallel; t) \\ = -\varepsilon \int_0^t [\xi_{mn}^z(\mathbf{k}_\perp + k_\parallel \hat{\mathbf{z}} + \varepsilon t' \hat{\mathbf{z}}) - \xi_{nn}^z(\mathbf{k}_\perp + k_\parallel \hat{\mathbf{z}} + \varepsilon t' \hat{\mathbf{z}})] dt'. \end{aligned} \quad (\text{B3})$$

From this equation we can write

$$\begin{aligned} \varphi_{mn}\left(\mathbf{k}_\perp, 0; t + \frac{k_\parallel}{\varepsilon}\right) \\ = -\varepsilon \int_0^{t+k_\parallel/\varepsilon} [\xi_{mn}^z(\mathbf{k}_\perp + \varepsilon t'' \hat{\mathbf{z}}) - \xi_{nn}^z(\mathbf{k}_\perp + \varepsilon t'' \hat{\mathbf{z}})] dt''. \end{aligned} \quad (\text{B4})$$

Introducing a new variable t' according to $t'' = t' + k_\parallel/\varepsilon$, when $t'' = 0$ we have $t' = -k_\parallel/\varepsilon$ and when $t'' = t + k_\parallel/\varepsilon$ we have $t' = t$, so

$$\begin{aligned} \varphi_{mn}\left(\mathbf{k}_\perp, 0; t + \frac{k_\parallel}{\varepsilon}\right) \\ = -\varepsilon \int_{-k_\parallel/\varepsilon}^0 [\xi_{mn}^z(\mathbf{k}_\perp + k_\parallel \hat{\mathbf{z}} + \varepsilon t' \hat{\mathbf{z}}) \\ - \xi_{nn}^z(\mathbf{k}_\perp + k_\parallel \hat{\mathbf{z}} + \varepsilon t' \hat{\mathbf{z}})] dt' \\ - \varepsilon \int_0^t [\xi_{mn}^z(\mathbf{k}_\perp + k_\parallel \hat{\mathbf{z}} + \varepsilon t' \hat{\mathbf{z}}) - \xi_{nn}^z(\mathbf{k}_\perp + k_\parallel \hat{\mathbf{z}} + \varepsilon t' \hat{\mathbf{z}})] dt' \\ = \sigma_{mn}(\mathbf{k}_\perp, k_\parallel) + \varphi_{mn}(\mathbf{k}_\perp, k_\parallel; t), \end{aligned}$$

where $\sigma_{mn}(\mathbf{k}_\perp, k_\parallel)$ is given by Eq. (43). Note

$$\begin{aligned} \sigma_{mn}(\mathbf{k}_\perp, 0) &= 0, \\ \sigma_{mn}(\mathbf{k}_\perp, k_\parallel) &= 0. \end{aligned} \quad (\text{B5})$$

From Eqs. (B1) and (B5) we can then write

$$\mathbf{V}_{mn}(\mathbf{k}_\perp, k_\parallel; t) = \mathbf{v}_{mn}[\mathbf{k}_\perp + \hat{\mathbf{z}}(k_\parallel + \varepsilon t)]e^{i\varphi_{mn}(\mathbf{k}_\perp, 0; t+k_\parallel/\varepsilon)}e^{-i\sigma_{mn}(\mathbf{k}_\perp, k_\parallel)} \quad (\text{B6})$$

while clearly

$$\mathbf{V}_{mn}\left(\mathbf{k}_\perp, 0; t + \frac{k_\parallel}{\varepsilon}\right) = \mathbf{v}_{mn}\left[\mathbf{k}_\perp + \hat{\mathbf{z}}\varepsilon\left(t + \frac{k_\parallel}{\varepsilon}\right)\right]e^{i\varphi_{mn}(\mathbf{k}_\perp, 0; t+k_\parallel/\varepsilon)} \quad (\text{B7})$$

so we find Eq. (42), identifying the link between $\mathbf{V}_{mn}(\mathbf{k}; t)$ for different \mathbf{k} and different t .

Similar relations hold for the components of $L(\mathbf{k}; t)$. We begin with Eq. (17), explicitly indicating \mathbf{k}_\perp and k_\parallel , $\boldsymbol{\mu}_{mn}(\mathbf{k}_\perp, k_\parallel; t) = \mathbf{e}_{\mathbf{r}_{mn}}[\mathbf{k}_\perp + \hat{\mathbf{z}}(k_\parallel + \varepsilon t)]e^{i\varphi_{mn}(\mathbf{k}_\perp, k_\parallel; t)}$. Now from this and the second of Eq. (36) we have

$$S_{pm}(\mathbf{k}_\perp, k_\parallel; t) = -e z_{pm} [\mathbf{k}_\perp + \hat{\mathbf{z}}(k_\parallel + \varepsilon t)] E_{dc} e^{i\varphi_{pm}(\mathbf{k}_\perp, k_\parallel; t)} \quad (\text{B8})$$

and so using Eq. (B5) we find

$$S_{pm}(\mathbf{k}_\perp, k_\parallel; t) = e^{-i\sigma_{pm}(\mathbf{k}_\perp, k_\parallel)} S_{pm}\left(\mathbf{k}_\perp, 0; t + \frac{k_\parallel}{\varepsilon}\right) \quad (\text{B9})$$

and from the first of Eq. (36) we find

$$T_{pm}(\mathbf{k}_\perp, k_\parallel; t) = e^{-i\sigma_{pm}(\mathbf{k}_\perp, k_\parallel)} T_{pm}\left(\mathbf{k}_\perp, 0; t + \frac{k_\parallel}{\varepsilon}\right), \quad (\text{B10})$$

where we have used the second of the identities (B5) and the fact that $T_{pm}(\mathbf{k}_\perp, k_\parallel; t)$ is diagonal.

These properties will allow us to establish a link between $L_{pn}(\mathbf{k}_\perp, k_\parallel; t)$ and $L_{pn}(\mathbf{k}_\perp, 0; t + k_\parallel/\varepsilon)$. Note that choosing $k_\parallel=0$ we can write Eq. (35) as

$$\begin{aligned} i\hbar \frac{dL_{pn}(\mathbf{k}_\perp, 0; t)}{dt} &= \sum_m [T_{pm}(\mathbf{k}_\perp, 0; t) + S_{pm}(\mathbf{k}_\perp, 0; t)] L_{mn}(\mathbf{k}_\perp, 0; t) \end{aligned} \quad (\text{B11})$$

so of course

$$\begin{aligned} i\hbar \frac{dL_{pn}\left(\mathbf{k}_\perp, 0; t + \frac{k_\parallel}{\varepsilon}\right)}{dt} &= \sum_m \left[T_{pm}\left(\mathbf{k}_\perp, 0; t + \frac{k_\parallel}{\varepsilon}\right) + S_{pm}\left(\mathbf{k}_\perp, 0; t + \frac{k_\parallel}{\varepsilon}\right) \right] \\ &\times L_{mn}\left(\mathbf{k}_\perp, 0; t + \frac{k_\parallel}{\varepsilon}\right) \end{aligned}$$

and so

$$\begin{aligned} i\hbar \frac{d\left[L_{pn}\left(\mathbf{k}_\perp, 0; t + \frac{k_\parallel}{\varepsilon}\right) e^{-i\sigma_{pn}(\mathbf{k}_\perp, k_\parallel)} \right]}{dt} &= \sum_m [T_{pm}(\mathbf{k}_\perp, k_\parallel; t) + S_{pm}(\mathbf{k}_\perp, k_\parallel; t)] \\ &\times \left[L_{mn}\left(\mathbf{k}_\perp, 0; t + \frac{k_\parallel}{\varepsilon}\right) e^{-i\sigma_{mn}(\mathbf{k}_\perp, k_\parallel)} \right], \end{aligned}$$

where we have used Eqs. (B9) and (B10), the fact that

$$\sigma_{pn}(\mathbf{k}_\perp, k_\parallel) = \sigma_{pm}(\mathbf{k}_\perp, k_\parallel) + \sigma_{mn}(\mathbf{k}_\perp, k_\parallel) \quad (\text{B12})$$

[see Eq. (43)] and the fact that the $\sigma_{pn}(\mathbf{k}_\perp, k_\parallel)$ are independent of time. But from Eq. (35) we have as well

$$\begin{aligned} i\hbar \frac{dL_{pn}(\mathbf{k}_\perp, k_\parallel; t)}{dt} &= \sum_m [T_{pm}(\mathbf{k}_\perp, k_\parallel; t) + S_{pm}(\mathbf{k}_\perp, k_\parallel; t)] L_{mn}(\mathbf{k}_\perp, k_\parallel; t) \end{aligned} \quad (\text{B13})$$

so we see that $L_{pn}(\mathbf{k}_\perp, k_\parallel; t)$ and

$L_{pn}(\mathbf{k}_\perp, 0; t + k_\parallel/\varepsilon) e^{-i\sigma_{pn}(\mathbf{k}_\perp, k_\parallel)}$ satisfy the same differential equation.

Defining $\hat{L}_{pn}(\mathbf{k}_\perp, k_\parallel; t)$ according to Eq. (45), and recalling that $\sigma_{pn}(\mathbf{k}_\perp, k_\parallel)$ is independent of time and satisfies the first of Eq. (B5), we see that $\hat{L}_{pn}(\mathbf{k}_\perp, k_\parallel; t)$ and $\hat{L}_{pn}(\mathbf{k}_\perp, 0; t + k_\parallel/\varepsilon)$ satisfy the same differential equation. Of course they need not be equal, because they can have different initial conditions; we turn to these in a moment. First, however, we consider a function $m_{pn}(\mathbf{k}_\perp; t)$ that satisfies Eq. (46) with initial condition given by Eq. (47). Then noting that $\hat{L}_{pn}(\mathbf{k}_\perp, 0; t)$ satisfies Eq. (B11), we can write

$$\hat{L}_{pn}(\mathbf{k}_\perp, 0; t) = \sum_q m_{pq}(\mathbf{k}_\perp; t) \mathcal{A}_{qn}(\mathbf{k}_\perp), \quad (\text{B14})$$

where the \mathcal{A}_{mn} are the components of a constant matrix that identifies the initial condition of $\hat{L}_{pn}(\mathbf{k}_\perp, 0; t)$; indeed, using Eq. (47) we see immediately that

$$\mathcal{A}_{mn}(\mathbf{k}_\perp) = \hat{L}_{mn}(\mathbf{k}_\perp, 0; 0). \quad (\text{B15})$$

Then since $\hat{L}_{pn}(\mathbf{k}_\perp, k_\parallel; t)$ and $\hat{L}_{pn}(\mathbf{k}_\perp, 0; t + k_\parallel/\varepsilon)$ satisfy the same differential equation we can write Eq. (44), where the $\mathcal{B}_{qn}(\mathbf{k}_\perp, k_\parallel)$ are the components of a constant matrix that, in a slightly more complicated way, encode the initial condition on $\hat{L}_{pn}(\mathbf{k}_\perp, k_\parallel; t)$.

Within the block approximation (see Sec. II F), Eq. (40) reduces to

$$\begin{aligned} \mathcal{N}'_c(t) &= \sum_{c, c', c'', \mathbf{k}_\perp, k_\parallel} L_{c'c}^*(\mathbf{k}_\perp, k_\parallel; t) L_{c''c}(\mathbf{k}_\perp, k_\parallel; t) \\ &\times \langle \Psi | b_{c' \mathbf{k}_\perp, k_\parallel}^\dagger b_{c'' \mathbf{k}_\perp, k_\parallel} | \Psi \rangle, \end{aligned} \quad (\text{B16})$$

where we have explicitly written the sum as one over both \mathbf{k}_\perp and k_\parallel , and used the block approximation. Using the fact that in the block approximation $L_{c'c}(\mathbf{k}_\perp, k_\parallel; t)$ (with the subscripts varying only over conduction band labels) is a unitary matrix, we recover Eq. (49).

To recover the form of our matrix $L(\mathbf{k}_\perp, k_\parallel; t)$, we write Eq. (48) as

$$\begin{aligned} L_{pn}(\mathbf{k}_\perp, k_\parallel; t) &= e^{-i\sigma_{pn}(\mathbf{k}_\perp, k_\parallel)} \sum_q m_{pq}\left(\mathbf{k}_\perp; t + \frac{k_\parallel}{\varepsilon}\right) \mathcal{B}_{qn}(\mathbf{k}_\perp, k_\parallel) \\ &= \sum_q \bar{m}_{pq}\left(\mathbf{k}_\perp; t + \frac{k_\parallel}{\varepsilon}\right) \bar{\mathcal{B}}_{qn}(\mathbf{k}_\perp, k_\parallel), \end{aligned} \quad (\text{B17})$$

where we have used Eq. (45) and where in the second line we used expressions of the form Eq. (B12), and have put

$$\begin{aligned} \bar{m}_{pq}\left(\mathbf{k}_\perp; t + \frac{k_\parallel}{\varepsilon}\right) &= e^{-i\sigma_{pq}(\mathbf{k}_\perp, k_\parallel)} m_{pq}\left(\mathbf{k}_\perp; t + \frac{k_\parallel}{\varepsilon}\right), \\ \bar{\mathcal{B}}_{qn}(\mathbf{k}_\perp, k_\parallel) &= e^{-i\sigma_{qn}(\mathbf{k}_\perp, k_\parallel)} \mathcal{B}_{qn}(\mathbf{k}_\perp, k_\parallel). \end{aligned} \quad (\text{B18})$$

It is easy to confirm that the $\bar{\mathcal{B}}_{qn}(\mathbf{k}_\perp, k_\parallel)$ are the elements of a unitary matrix.

APPENDIX C: CALCULATION OF $|\Psi^{(1)}\rangle$ IN THE PRESENCE OF A dc FIELD

We now turn to the evaluation of the interaction Hamiltonian and the identification of the necessary matrix elements. From Eq. (33) we have

$$\begin{aligned} \tilde{\mathcal{J}}(t) = & e \sum_{\mathbf{k}_\perp, k_\parallel} \sum_{n_1, n_2} \sum_{a, b} b_{n_2 \mathbf{k}_\perp k_\parallel}^\dagger b_{n_1 \mathbf{k}_\perp k_\parallel} L_{an_2}^*(\mathbf{k}_\perp, k_\parallel; t) \\ & \times \mathbf{V}_{ab}(\mathbf{k}_\perp, k_\parallel; t) L_{bn_1}(\mathbf{k}_\perp, k_\parallel; t), \end{aligned}$$

where we have used Eq. (34) for $\tilde{\mathbf{V}}_{n_2 n_1}(\mathbf{k}; t)$, and we explicitly indicate the dependence on \mathbf{k}_\perp and k_\parallel . When we use this in perturbation theory we will only be interested in the terms in the summations that do not destroy the state $|\Psi^H\rangle$ and which produce an excited state. Thus we demand that n_1 is a valence state and n_2 a conduction state. Recalling the block diagonal form [Eq. (48)] assumed for $L(\mathbf{k}; t)$, we can write

$$\begin{aligned} \tilde{\mathcal{J}}(t) = & e \sum_{\mathbf{k}_\perp, k_\parallel} \sum_{v, c} \sum_{c', v'} b_{c \mathbf{k}_\perp k_\parallel}^\dagger b_{v \mathbf{k}_\perp k_\parallel} L_{c'c}^*(\mathbf{k}_\perp, k_\parallel; t) \\ & \times \mathbf{V}_{c'v'}(\mathbf{k}_\perp, k_\parallel; t) L_{v'v}(\mathbf{k}_\perp, k_\parallel; t). \end{aligned}$$

Using Eq. (B17) this becomes

$$\begin{aligned} \tilde{\mathcal{J}}(t) = & e \sum_{\mathbf{k}_\perp, k_\parallel} \sum_{v'', c''} \sum_{c', v'} \bar{m}_{c'c''}^* \left(\mathbf{k}_\perp; t + \frac{k_\parallel}{\varepsilon} \right) \\ & \times \mathbf{V}_{c'v'}(\mathbf{k}_\perp, k_\parallel; t) \bar{m}_{v'v''} \left(\mathbf{k}_\perp; t + \frac{k_\parallel}{\varepsilon} \right) \\ & \times \left[\sum_c \bar{B}_{c''c}^*(\mathbf{k}_\perp, k_\parallel) b_{c \mathbf{k}_\perp k_\parallel}^\dagger \right] \left[\sum_v \bar{B}_{v''v}(\mathbf{k}_\perp, k_\parallel) b_{v \mathbf{k}_\perp k_\parallel} \right]. \end{aligned}$$

Defining

$$\begin{aligned} B_{v'' \mathbf{k}_\perp k_\parallel} &= \sum_v \bar{B}_{v''v}(\mathbf{k}_\perp, k_\parallel) b_{v \mathbf{k}_\perp k_\parallel}, \\ B_{c'' \mathbf{k}_\perp k_\parallel} &= \sum_c \bar{B}_{c''c}^*(\mathbf{k}_\perp, k_\parallel) b_{c \mathbf{k}_\perp k_\parallel} \end{aligned} \quad (\text{C1})$$

we have

$$\begin{aligned} \tilde{\mathcal{J}}(t) = & e \sum_{\mathbf{k}_\perp, k_\parallel} \sum_{v'', c''} \sum_{c', v'} \bar{m}_{c'c''}^* \left(\mathbf{k}_\perp; t + \frac{k_\parallel}{\varepsilon} \right) \\ & \times \mathbf{V}_{c'v'}(\mathbf{k}_\perp, k_\parallel; t) \bar{m}_{v'v''} \left(\mathbf{k}_\perp; t + \frac{k_\parallel}{\varepsilon} \right) B_{c'' \mathbf{k}_\perp k_\parallel}^\dagger B_{v'' \mathbf{k}_\perp k_\parallel} \\ = & e \sum_{\mathbf{k}_\perp, k_\parallel} \sum_{v'', c''} e^{-i\sigma_{c''v''}(\mathbf{k}_\perp, k_\parallel)} \mathbf{F}_{c''v''} \left(\mathbf{k}_\perp; t + \frac{k_\parallel}{\varepsilon} \right) B_{c'' \mathbf{k}_\perp k_\parallel}^\dagger B_{v'' \mathbf{k}_\perp k_\parallel}, \end{aligned}$$

where

$$\begin{aligned} \mathbf{F}_{c''v''} \left(\mathbf{k}_\perp; t + \frac{k_\parallel}{\varepsilon} \right) = & \sum_{c', v'} m_{c'c''}^* \left(\mathbf{k}_\perp; t + \frac{k_\parallel}{\varepsilon} \right) \\ & \times \mathbf{V}_{c'v'} \left(\mathbf{k}_\perp, 0; t + \frac{k_\parallel}{\varepsilon} \right) m_{v'v''} \left(\mathbf{k}_\perp; t + \frac{k_\parallel}{\varepsilon} \right) \end{aligned} \quad (\text{C2})$$

and we have used the first of Eqs. (42) and (B18).

We now study the properties of the operators $B_{v \mathbf{k}_\perp k_\parallel}$ and $B_{c \mathbf{k}_\perp k_\parallel}$. From the fact that the operators $b_{n \mathbf{k}_\perp k_\parallel}$ and their adjoints satisfy the fundamental anticommutation relations, it is clear that

$$\{B_{n \mathbf{k}_\perp k_\parallel}, B_{m \mathbf{k}'_\perp k'_\parallel}\} = \{B_{n \mathbf{k}_\perp k_\parallel}, B_{m \mathbf{k}'_\perp k'_\parallel}^\dagger\} = 0 \quad (\text{C3})$$

if $\mathbf{k}_\perp + k_\parallel \hat{z} \neq \mathbf{k}'_\perp + k'_\parallel \hat{z}$. To investigate the case where $\mathbf{k}_\perp + k_\parallel \hat{z} = \mathbf{k}'_\perp + k'_\parallel \hat{z}$ we can then drop the \mathbf{k}_\perp and k_\parallel subscripts. Also it is clear that B_c anticommutes with B_v and B_v^\dagger , and that B_v anticommutes with B_c^\dagger as well. So we need only investigate the anticommutation relations of B_n and B_m^\dagger , where n and m are either both conduction labels or both valence labels. Since the $\bar{B}_{v''v}(\mathbf{k}_\perp, k_\parallel)$ and the $\bar{B}_{c''c}(\mathbf{k}_\perp, k_\parallel)$ are respectively elements of unitary matrices, we have

$$\{B_m, B_n^\dagger\} = \sum_{p, q} \bar{B}_{mp} \bar{B}_{nq}^* \{b_p, b_q^\dagger\} = \sum_{p, q} \bar{B}_{mp} \bar{B}_{nq}^* \delta_{pq} = \delta_{mn}.$$

So then we see that our full set of operators are fermion operators. Restoring the full notation, we have

$$\begin{aligned} \{B_{n \mathbf{k}_\perp k_\parallel}, B_{m \mathbf{k}'_\perp k'_\parallel}\} &= \{B_{n \mathbf{k}_\perp k_\parallel}, B_{m \mathbf{k}'_\perp k'_\parallel}^\dagger\} = 0, \\ \{B_{n \mathbf{k}_\perp k_\parallel}, B_{m \mathbf{k}'_\perp k'_\parallel}^\dagger\} &= \delta_{nm} \delta_{\mathbf{k}_\perp \mathbf{k}'_\perp} \delta_{k_\parallel k'_\parallel}. \end{aligned} \quad (\text{C4})$$

Further, from Eqs. (29) and (30) and the definitions in Eq. (C1) we see that we have

$$\begin{aligned} B_{c \mathbf{k}_\perp k_\parallel} |\Psi^H\rangle &= 0, \\ B_{v \mathbf{k}_\perp k_\parallel}^\dagger |\Psi^H\rangle &= 0 \end{aligned}$$

and we can understand our initial state as filled with fermions identified by the operators labeled $v \mathbf{k}_\perp k_\parallel$, and empty of the fermions identified by the operators labeled $c \mathbf{k}_\perp k_\parallel$. These “new fermion states” are just linear combinations of our old fermion states, where the new conduction band states involve only old conduction band states, and the new valence band states involve only old valence band states.

Thus we can identify

$$\overline{|c''v''(\mathbf{k}_\perp k_\parallel)\rangle} = e^{-i\sigma_{c''v''}(\mathbf{k}_\perp, k_\parallel)} B_{c'' \mathbf{k}_\perp k_\parallel}^\dagger B_{v'' \mathbf{k}_\perp k_\parallel} |\Psi^H\rangle \quad (\text{C5})$$

as a state where there is one electron removed from the valence bands and one deposited in the conduction bands; it is convenient to include the phase factor in the definition of the state. From the fundamental anticommutation relations [Eq. (C4)] we have Eq. (55). Finally, note that the effect of our operator $\tilde{\mathcal{J}}(t)$ [Eq. (33)] on our Heisenberg ket can be written as

$$\tilde{\mathcal{J}}(t)|\Psi^H\rangle = e \sum_{\mathbf{k}_\perp, k_\parallel} \sum_{v,c} \mathbf{F}_{cv} \left(\mathbf{k}_\perp; t + \frac{k_\parallel}{\varepsilon} \right) \overline{|cv(\mathbf{k}_\perp, k_\parallel)\rangle} \quad (\text{C6})$$

and so we have

$$|\Psi^{(1)}\rangle = -\frac{e}{i\hbar c} \sum_{\mathbf{k}_\perp, k_\parallel} \sum_{v,c} \int_{-\infty}^{\infty} \mathbf{F}_{cv} \left(\mathbf{k}_\perp; t + \frac{k_\parallel}{\varepsilon} \right) \cdot \mathbf{A}_{\text{opt}}(t) \overline{|cv(\mathbf{k}_\perp, k_\parallel)\rangle} dt. \quad (\text{C7})$$

Fourier expanding the optical pulse

$$\mathbf{A}_{\text{opt}}(t) = \int \frac{d\omega}{2\pi} \mathbf{A}(\omega) e^{-i\omega t} \quad (\text{C8})$$

and using

$$\mathbf{E}(\omega) = \frac{i\omega \mathbf{A}(\omega)}{c} \quad (\text{C9})$$

we have

$$\begin{aligned} |\Psi^{(1)}\rangle &= \frac{e}{2\pi\hbar} \sum_{\mathbf{k}_\perp, k_\parallel} \sum_{v,c} \int d\omega \frac{\mathbf{E}_{\text{opt}}(\omega)}{\omega} \\ &\quad \cdot \int_{-\infty}^{\infty} \mathbf{F}_{cv} \left(\mathbf{k}_\perp; t + \frac{k_\parallel}{\varepsilon} \right) e^{-i\omega t} \overline{|cv(\mathbf{k}_\perp, k_\parallel)\rangle} dt \\ &= \frac{e}{2\pi\hbar} \sum_{\mathbf{k}_\perp, k_\parallel} \sum_{v,c} \int d\omega \frac{\mathbf{E}_{\text{opt}}(\omega)}{\omega} e^{i\omega k_\parallel/\varepsilon} \\ &\quad \cdot \int_{-\infty}^{\infty} \mathbf{F}_{cv} \left(\mathbf{k}_\perp; t + \frac{k_\parallel}{\varepsilon} \right) e^{-i\omega(t+k_\parallel/\varepsilon)} \overline{|cv(\mathbf{k}_\perp, k_\parallel)\rangle} dt \\ &= \frac{e}{2\pi\hbar} \sum_{\mathbf{k}_\perp, k_\parallel} \sum_{v,c} \int d\omega \frac{\mathbf{F}_{cv}(\mathbf{k}_\perp; -\omega)}{\omega} \\ &\quad \cdot \mathbf{E}_{\text{opt}}(\omega) e^{i\omega k_\parallel/\varepsilon} \overline{|cv(\mathbf{k}_\perp, k_\parallel)\rangle}, \end{aligned}$$

where $\mathbf{F}_{cv}(\mathbf{k}_\perp; -\omega)$ is given by Eq. (52). This leads to Eq. (50).

To now calculate the expectation value of the number of carriers injected into the conduction bands, we can use Eq. (49). Since the second of Eq. (C1) identifies a unitary transformation between the $B_{c\mathbf{k}_\perp, k_\parallel}$ and the $b_{c\mathbf{k}_\perp, k_\parallel}$, we can just as well write

$$N_c = \sum_{c, \mathbf{k}_\perp, k_\parallel} B_{c\mathbf{k}_\perp, k_\parallel}^\dagger B_{c\mathbf{k}_\perp, k_\parallel}. \quad (\text{C10})$$

Using this it is clear that $|\Psi^{(1)}\rangle$ [see Eq. (50)] is an eigenket of N_c with eigenvalue unity ($N_c|\Psi^{(1)}\rangle = |\Psi^{(1)}\rangle$).

APPENDIX D: ABSORPTION IN THE ABSENCE OF A dc FIELD

For reference and to have a result in the same notation as our main calculation, we sketch here the usual derivation of absorption in the absence of a dc field. Here we can take $\mathbf{A}_{\text{dc}}(t)=0$ for all times, and hence \mathbf{K}^o [see Eq. (22)] can be taken to vanish. The evolution in Eq. (20) then holds for all times and we can take

$$L_{mp}(\mathbf{k}; t) = \delta_{mp} e^{-i\omega_m(\mathbf{k})t}. \quad (\text{D1})$$

Using this in Eq. (40) we have

$$\mathcal{N}_c = \sum_{c, \mathbf{k}} \langle \Psi | b_{c\mathbf{k}}^\dagger b_{c\mathbf{k}} | \Psi \rangle \quad \text{for } t > t_{\text{end}} \quad (\text{D2})$$

with $|\Psi\rangle$ given by Eq. (37) at times after the pulse has passed. To evaluate it we use $\tilde{\mathbf{V}}_{nq}(\mathbf{k}; t) = \mathbf{v}_{nq}(\mathbf{k}) e^{i\omega_{nq}(\mathbf{k})t}$, which follows from Eqs. (15) and (34) in the absence of a dc field, and Eq. (D1), in the expressions (32) and (33) for $H_{\text{eff}}(t)$ to yield

$$H_{\text{eff}}(t) = -\frac{e}{c} \sum_{c, n, q, \mathbf{k}} b_{n\mathbf{k}}^\dagger b_{q\mathbf{k}} \mathbf{v}_{nq}(\mathbf{k}) \cdot \mathbf{A}_{\text{opt}}(t) e^{i\omega_{nq}(\mathbf{k})t}.$$

When this acts on $|\Psi^H\rangle$ we will get, other than a term proportional to $|\Psi^H\rangle$ itself which will not contribute to carrier injection to lowest order, a contribution only if q is a valence band and n is a conduction band. So from Eq. (38) we find

$$|\Psi^{(1)}\rangle = -\frac{e}{i\hbar c} \sum_{c, v, \mathbf{k}} \int_{-\infty}^{\infty} dt \mathbf{v}_{cv}(\mathbf{k}) \cdot \mathbf{A}_{\text{opt}}(t) e^{i\omega_{cv}(\mathbf{k})t} |cv(\mathbf{k})\rangle,$$

where the state

$$|cv(\mathbf{k})\rangle = b_{c\mathbf{k}}^\dagger b_{v\mathbf{k}} |\Psi^H\rangle. \quad (\text{D3})$$

Fourier expanding the optical pulse according to Eq. (C8), and writing the result in terms of $\mathbf{E}(\omega)$ according to Eq. (C9), we find

$$|\Psi^{(1)}\rangle = \sum_{c, v, \mathbf{k}} \int d\omega \gamma_{cv\mathbf{k}}^j E^i(\omega) \delta[\omega - \omega_{cv}(\mathbf{k})] |cv(\mathbf{k})\rangle,$$

where $\gamma_{cv\mathbf{k}}^j$ is given by Eq. (61). Here $|\Psi^{(1)}\rangle$ is easily confirmed to be an eigenstate of the conduction band number operator

$$N_c = \sum_{c, \mathbf{k}} b_{c\mathbf{k}}^\dagger b_{c\mathbf{k}}$$

with eigenvalue unity, $N_c|\Psi^{(1)}\rangle = |\Psi^{(1)}\rangle$, and so as in the calculation with the dc field present we have Eq. (56), and using the property $\langle c'v'(\mathbf{k}') | cv(\mathbf{k}) \rangle = \delta_{c',c} \delta_{v',v} \delta_{\mathbf{k}',\mathbf{k}}$ of the states Eq. (D3) we find

$$N_c = \sum_{c, v, \mathbf{k}} \int_0^{\infty} d\omega \gamma_{cv\mathbf{k}}^j (\gamma_{cv\mathbf{k}}^j)^* E^i(\omega) [E^j(\omega)]^* \delta[\omega - \omega_{cv}(\mathbf{k})], \quad (\text{D4})$$

where we need only integrate over positive frequencies because $\omega_{cv}(\mathbf{k}) > 0$. Converting the sum over \mathbf{k} to an integral, putting $n = N_c/\Omega$, and then moving to the Fermi's golden rule limit, we find Eq. (60).

APPENDIX E: FKE FOR PARABOLIC, UNCOUPLED BANDS

In this appendix we verify that our calculation reduces to the analytical Airy function theory for the case of two parabolic bands and constant matrix elements. We consider band energies of the form

$$\hbar\omega_c(\mathbf{k}) = \hbar\omega_g + \frac{\hbar^2 k^2}{2m_c} \quad \text{and} \quad \hbar\omega_v(\mathbf{k}) = -\frac{\hbar^2 k^2}{2m_v}, \quad (\text{E1})$$

where m_c is the electron mass, m_v is the hole mass, and $\hbar\omega_g$ is the band-gap energy. We assume that the interband velocity matrix element is a constant \mathbf{V}_{cv} throughout the Brillouin zone.

Since there is only one valence band and one conduction band, and we neglect Zener tunneling between the two, Eq. (46) simplifies considerably. Since $S=0$ and T is diagonal, one can write down the solution

$$m_{pn}(\mathbf{k}_\perp; t) = \delta_{pn} \exp \left[i \int_0^t \omega_p(\mathbf{k}_\perp; t') dt' \right]. \quad (\text{E2})$$

Putting Eq. (E1) into Eq. (E2) and then using that and $k_\parallel = \varepsilon t$ in Eqs. (52) and (53), we have

$$\mathbf{F}_{cv}(\mathbf{k}_\perp; -\omega) = \mathbf{V}_{cv} \int_{-\infty}^{\infty} \frac{dt}{2\pi} e^{i(-\omega t + \omega_g t + \hbar k_\perp^2 t / 2\mu_{cv} + \hbar \varepsilon^2 t^3 / 6\mu_{cv})},$$

where $\mu_{cv} \equiv 1/(m_c^{-1} + m_v^{-1})$ is the reduced mass. Now let $s^3 = \hbar \varepsilon^2 t^3 / (2\mu_{cv})$, define the electro-optic frequency $\Omega_{cv} \equiv (\hbar \varepsilon^2 / 2\mu_{cv})^{1/3}$, and using the integral definition of the Airy function $\text{Ai}(x)$, we find

$$\mathbf{F}_{cv}(\mathbf{k}_\perp; -\omega) = \frac{\mathbf{V}_{cv}}{\Omega_{cv}} \text{Ai} \left(-\frac{\omega - \omega_g - \hbar k_\perp^2 / 2\mu_{cv}}{\Omega_{cv}} \right). \quad (\text{E3})$$

Using the above in Eqs. (51) and (59) and integrating over \mathbf{k}_\perp , using a few Airy function identities, and specializing to $i=j$, we find Eq. (64), the familiar expression for the electro-absorption with parabolic bands at an M_0 critical point in the limit of no broadening.³

*Present address: Department of Physics, University of Maryland, College Park, MD 20742, USA; wahlstrj@umd.edu

†Permanent address: Department of Physics, University of Toronto, Toronto, Ontario, Canada M5S1A7.

¹W. Franz, Z. Naturforsch. A **13**, 484 (1958).

²L. V. Keldysh, Sov. Phys. JETP **7**, 788 (1958).

³D. E. Aspnes, Phys. Rev. **147**, 554 (1966).

⁴D. E. Aspnes, Phys. Rev. **153**, 972 (1967).

⁵B. Knüpfer, P. Kiesel, M. Kneissl, S. Dankowski, N. Linder, G. Weimann, and G. Döhler, IEEE Photon. Technol. Lett. **5**, 1386 (1993).

⁶D. E. Aspnes and J. E. Rowe, Phys. Rev. B **5**, 4022 (1972).

⁷H. Shen and M. Dutta, J. Appl. Phys. **78**, 2151 (1995), and references therein.

⁸J. Hader, N. Linder, and G. H. Döhler, Phys. Rev. B **55**, 6960 (1997).

⁹D. E. Aspnes, Phys. Rev. B **10**, 4228 (1974).

¹⁰D. E. Aspnes, Phys. Rev. B **12**, 2297 (1975).

¹¹L. V. Keldysh, O. V. Konstantinov, and V. I. Perel', Sov. Phys. Semicond. **3**, 876 (1970).

¹²R. Enderlein, P. Renner, and M. Scheele, Phys. Status Solidi B **71**, 503 (1975).

¹³N. Bottka and J. E. Fischer, Phys. Rev. B **3**, 2514 (1971).

¹⁴V. Rehn, Surf. Sci. **37**, 443 (1973).

¹⁵D. F. Blossey, Phys. Rev. B **2**, 3976 (1970).

¹⁶D. F. Blossey, Phys. Rev. B **3**, 1382 (1971).

¹⁷A. Jaeger, G. Weiser, P. Wiedemann, I. Gyuro, and E. Zielinski, J. Phys.: Condens. Matter **8**, 6779 (1996).

¹⁸M. Lax, Symmetry Principles in Solid State and Molecular Physics (Dover, New York, 1974).

¹⁹J. E. Sipe and E. Ghahramani, Phys. Rev. B **48**, 11705 (1993).

²⁰P. Yu and M. Cardona, Fundamentals of Semiconductors, 2nd ed. (Springer-Verlag, Berlin, 1999).

²¹D. E. Aspnes, P. Handler, and D. F. Blossey, Phys. Rev. **166**, 921 (1968).

²²M. Cardona, F. Pollak, and J. Broerman, Phys. Lett. **19**, 276 (1965).

²³P. Pfeffer and W. Zawadzki, Phys. Rev. B **53**, 12813 (1996).

²⁴R. Winkler, Spin-Orbit Coupling Effects in Two-Dimensional Electron and Hole Systems, Springer Tracts in Modern Physics Vol. 191 (Springer, Berlin, 2003).

²⁵U. Rössler, Solid State Commun. **49**, 943 (1984).

²⁶P. Pfeffer and W. Zawadzki, Phys. Rev. B **41**, 1561 (1990).

²⁷H. Mayer and U. Rössler, Phys. Rev. B **44**, 9048 (1991).

²⁸H. Mayer and U. Rössler, Solid State Commun. **87**, 81 (1993).

²⁹H. Mayer, U. Rössler, and M. Ruff, Phys. Rev. B **47**, 12929 (1993).

³⁰R. D. R. Bhat, F. Nastos, A. Najmaie, and J. E. Sipe, Phys. Rev. Lett. **94**, 096603 (2005).

³¹R. Bhat and J. Sipe, arXiv:cond-mat/0601277 (unpublished).

³²P. Löwdin, J. Chem. Phys. **19**, 1396 (1951).

³³M. Cardona, N. E. Christensen, and G. Fasol, Phys. Rev. B **38**, 1806 (1988).

³⁴A. Baldereschi and N. O. Lipari, Phys. Rev. B **8**, 2697 (1973).

³⁵P. Enders, A. Bärwolff, M. Woerner, and D. Suisky, Phys. Rev. B **51**, 16695 (1995).

³⁶P. Handler, S. Jaspersen, and S. Koeppen, Phys. Rev. Lett. **23**, 1387 (1969).

³⁷C. Van Hoof, K. Deneffe, J. De Boeck, D. J. Arent, and G. Borghs, Appl. Phys. Lett. **54**, 608 (1989).

³⁸M. Ruff, D. Streb, S. U. Dankowski, S. Tautz, P. Kiesel, B. Knüpfer, M. Kneissl, N. Linder, G. H. Döhler, and U. D. Keil, Appl. Phys. Lett. **68**, 2968 (1996).

³⁹J. E. Fischer and N. Bottka, Phys. Rev. Lett. **24**, 1292 (1970).

⁴⁰J. B. Khurgin and P. Voisin, Semicond. Sci. Technol. **12**, 1378 (1997).

⁴¹J. B. Khurgin and P. Voisin, Phys. Rev. Lett. **81**, 3777 (1998).

⁴²B. A. Foreman, J. Phys.: Condens. Matter **12**, R435 (2000).

⁴³B. A. Foreman, Phys. Rev. Lett. **84**, 2505 (2000).

⁴⁴M. Chang and Q. Niu, J. Phys.: Condens. Matter **20**, 193202 (2008).

⁴⁵D. Culcer, Y. Yao, and Q. Niu, Phys. Rev. B **72**, 085110 (2005).

⁴⁶A. Jaeger and G. Weiser, Phys. Rev. B **58**, 10674 (1998).

⁴⁷D. E. Aspnes and A. A. Studna, Phys. Rev. B **7**, 4605 (1973).

⁴⁸H. J. Kolbe, C. Agert, W. Stolz, and G. Weiser, Phys. Rev. B **59**, 14896 (1999).

- ⁴⁹V. Alperovich, A. Jaroshevich, H. Scheibler, and A. Terekhov, *Solid-State Electron.* **37**, 657 (1994).
- ⁵⁰P. Jin, S. H. Pan, Y. G. Li, C. Z. Zhang, and Z. G. Wang, *Semicond. Sci. Technol.* **21**, 786 (2006).
- ⁵¹P. Jin, S. H. Pan, and J. B. Liang, *J. Appl. Phys.* **88**, 6429 (2000).
- ⁵²J. K. Wahlstrand, H. Zhang, and S. T. Cundiff, *Appl. Phys. Lett.* **96**, 101104 (2010).
- ⁵³A. G. Aronov and G. E. Pikus, *Sov. Phys. Solid State* **10**, 648 (1968).
- ⁵⁴T. G. Pedersen and T. B. Lyngø, *J. Phys.: Condens. Matter* **15**, 3813 (2003).
- ⁵⁵D. S. Kyser and V. Rehn, *Solid State Commun.* **8**, 1437 (1970).
- ⁵⁶S. E. Acosta-Ortiz and A. Lastras-Martínez, *Phys. Rev. B* **40**, 1426 (1989).
- ⁵⁷D. A. Belogurov and Y. V. Shaldin, *Sov. Phys. Semicond.* **10**, 1007 (1976).
- ⁵⁸R. Del Sole and D. E. Aspnes, *Phys. Rev. B* **17**, 3310 (1978).
- ⁵⁹D. E. Aspnes and A. A. Studna, *Phys. Rev. Lett.* **54**, 1956 (1985).
- ⁶⁰R. Del Sole, W. L. Mochan, and R. G. Barrera, *Phys. Rev. B* **43**, 2136 (1991).
- ⁶¹L. F. Lastras-Martínez and A. Lastras-Martínez, *Phys. Rev. B* **54**, 10726 (1996).
- ⁶²J. M. Fraser, A. I. Shkrebti, J. E. Sipe, and H. M. van Driel, *Phys. Rev. Lett.* **83**, 4192 (1999).
- ⁶³C. Xia and H. N. Spector, *J. Appl. Phys.* **105**, 084313 (2009).
- ⁶⁴A. Schwanhäußer, M. Betz, M. Eckardt, S. Trumm, L. Robledo, S. Malzer, A. Leitenstorfer, and G. H. Döhler, *Phys. Rev. B* **70**, 085211 (2004).
- ⁶⁵H. Heesel, S. Hunsche, H. Mikkelsen, T. Dekorsy, K. Leo, and H. Kurz, *Phys. Rev. B* **47**, 16000 (1993).